

We thank the reviewers for carefully reading and providing comments to improve our manuscript. Each point made by the reviewers is given as bold with our responses given in plain text. Specific lines in the manuscript are quoted with changes marked in red.

Reviewer #1

The study by Jen et al. evaluates the capabilities of two different primary ions (nitrate and acetate) in ionizing clusters composed of sulfuric acid and dimethylamine (DMA), ethylene diamine (EDA), tetramethylethylene (TMEDA), or butanediamine/putrescine (PUT). Such clusters could in principle explain atmospheric new particle formation (NPF) since the produced neutral clusters have low evaporation rates.

The neutral clusters were formed in a flow reactor at ~300 K and at 30% relative humidity. A chemical ionization mass spectrometer (cluster CIMS) was used to detect the clusters after they reacted with nitrate or acetate primary ions used for the chemical ionization. Since the formed neutral clusters can contain equal numbers of acid and base molecules their reduced acidity could make them less susceptible towards ionization by nitrate in comparison to acetate primary ions.

Indeed, the presented results indicate that some clusters can very likely not be ionized efficiently by nitrate (e.g. the sulfuric acid dimer containing two diamines, or the trimer containing DMA or diamines).

In atmospheric studies nitrate chemical ionization is generally used for measuring sulfuric acid and its influence on NPF. If some atmospheric NPF is due to sulfuric acid and amines or diamines its importance could be significantly underestimated because the absence of sulfuric acid clusters would not necessarily indicate that sulfuric acid-amine NPF is not proceeding.

For this reason the manuscript by Jen et al. is a very important contribution and will help the interpretation of the mass spectra obtained in ambient and chamber CIMS measurements. The paper is very well-written and I have no serious comments. I therefore recommend its publication after addressing the points listed in the following:

Line 31: add a space before the bracket and also between the references (after the semicolon, please check the whole manuscript)

Thank you for pointing this out. We have made every effort to correct these typos.

Line 145: opening bracket is missing before Am.B2

The bracket has been added.

Line 171: “factor of 2 below”, does this mean all concentrations are upper estimates?

All the reported acetate concentrations represent an upper estimate. This is due to the uncertainty in the mass dependent sensitivity of for the smallest ions, including the acetate reagent ions. We have rephrased this sentence for clarity

“The systematic uncertainties of the acetate measurement are due to similar reasons as those for $[N_1]$ and could lead to a factor of 2-3 times lower $[N_2]$ than reported here.”

Figure 2: By comparing the panels a) and b) for the trimer it is not clear why the trimer in panel b) is >10 times higher for acetate than for nitrate. The trimer signals in panel a) are dominated by the cluster containing 3 acids and 1 base, however these signals seem to be quite similar for acetate and nitrate.

We sincerely apologize for this graphical mistake. We have fixed Figure 2 and clarified the corresponding sentence in the text.

“For all bases, the measured $[N_3]$ by acetate is 2 to 100 times higher than concentrations measured by nitrate CI.”

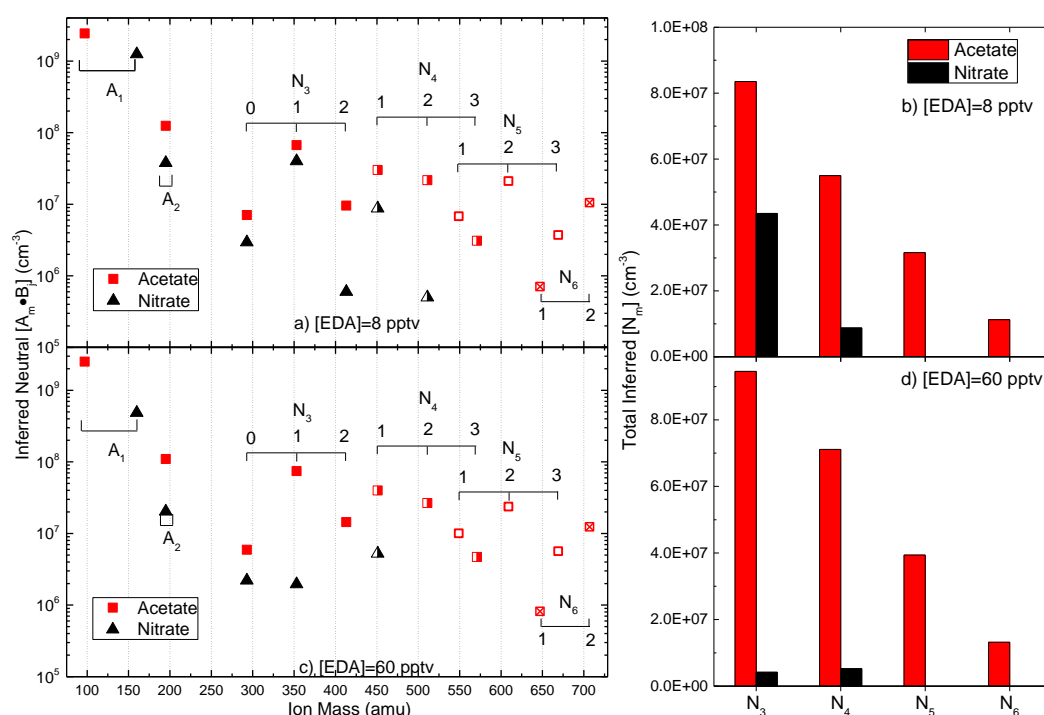


Figure 4: This figure seems to show signals for $A^- \cdot \text{Put}$, which is surprising given the fact that in the DMA system, $A^- \cdot \text{DMA}$ evaporates very rapidly. It would be good to include some discussion about the presence of $A^- \cdot \text{Put}$.

The reviewer points out a very interesting observation. We have wondered about this rather bizarre sighting of an aminated monomer. We do not see $A_1^- \cdot \text{EDA}$ or $A_1^- \cdot \text{TMEDA}$ either. Elm et al. (2016) very recently published free energies of sulfuric acid+diamine clusters. Though they did not model ions, the formation free energies of $A_1 \cdot \text{Put}$ is lower at -15.4 kcal/mol than $A_1 \cdot \text{EDA}$ at -11.1 kcal/mol; TMEDA was not modeled. $A_1 \cdot \text{DMA}$ binding energy is -11.4 kcal/mol and is much closer to $A_1 \cdot \text{EDA}$. It is likely that the very strong binding energies of $A_1 \cdot \text{Put}$ could mean that $A_1^- \cdot \text{Put}$ will survive until detection. More computational chemistry studies are needed to conclude this is the case.

Per the reviewer's suggestion, we have added a short paragraph discussing this.

“Unlike the other bases, Put was observed in the monomer using either nitrate or acetate CI (Figure 4). The presence of $A_1^- \bullet \text{Put}$ indicates its binding energy must be higher than monomers containing the other bases. However, this ion still decomposes in roughly the $t_{CI}=15$ ms as it is $\sim 0.1\%$ of $[N_1]$. Elm et al. (2016) has shown that the binding energy of $A_1^- \bullet \text{EDA}$ is -11.1 kcal/mol and $A_1^- \bullet \text{Put}$ is -15.4 kcal/mol, with $A_1^- \bullet \text{DMA}$ closely matching $A_1^- \bullet \text{EDA}$ at -11.38 kcal/mol (Nadykto et al., 2014; Bork et al., 2014). The higher neutral binding energies of $A_1^- \bullet \text{Put}$ may translate to stronger ion binding energies than the other aminated monomers, though more studies are needed to confirm this.”

Line 249 and SI equation S6: Equation S6 includes the difference between k_{21} (reaction between H_2SO_4 and HSO_4^-) and k_1 (reaction between H_2SO_4 and NO_3^-) in the denominator of the equation. It seems that these values are identical ($2 \times 10^{-9} \text{ cm}^3 \text{ s}^{-1}$), therefore this would lead to a zero division. Please clarify.

The reviewer noticed an interesting point for equation S6. Two responses to this:

- 1) The forward rate constants used to invert Cluster CIMS signals to neutral cluster concentrations were not assumed to be all $2 \times 10^{-9} \text{ cm}^3 \text{ s}^{-1}$. For signal inversion, we used $k_1 = 1.9 \times 10^{-9} \text{ cm}^3 \text{ s}^{-1}$ and $k_{21} = 2 \times 10^{-9} \text{ cm}^3 \text{ s}^{-1}$. For the model, we used all forward rate constants as $2 \times 10^{-9} \text{ cm}^3 \text{ s}^{-1}$, but the model does not follow Equation S6 as it numerically solves all the cluster balance equations.
- 2) Equation S6 is a bit more complicated than $k_{21}-k_1$ in the denominator. This equation can be re-written as

$$\frac{[A_1^-]}{[NO_3^-]} = \frac{S_{160}}{S_{125}} = \frac{k_1}{k_{21} - k_1} \left(1 - \exp(-(k_{21} - k_1)[N_1]t_{CI}) \right)$$

As $k_{21}-k_1$ becomes very small, we can do a Taylor series expansion on the exponential.

$$x = -(k_{21} - k_1)[N_1]t_{Cl}$$

$$\frac{[A_1^-]}{[NO_3^-]} = \frac{k_1}{k_{21} - k_1} \left(1 - \left(1 + x + \frac{x^2}{2} \right) \right)$$

$$\frac{[A_1^-]}{[NO_3^-]} = \frac{-k_1}{k_{21} - k_1} \left(x + \frac{x^2}{2} \right)$$

$$\frac{[A_1^-]}{[NO_3^-]} = \frac{-k_1}{k_{21} - k_1} \left(-(k_{21} - k_1)[N_1]t_{Cl} + \frac{(-(k_{21} - k_1)[N_1]t_{Cl})^2}{2} \right)$$

$$\frac{[A_1^-]}{[NO_3^-]} = \left((k_1[N_1]t_{Cl}) + \frac{k_1(k_{21} - k_1)([N_1]t_{Cl})^2}{2} \right)$$

$$\lim_{k_{21} - k_1 \rightarrow 0} \frac{[A_1^-]}{[NO_3^-]} = (k_1[N_1]t_{Cl})$$

Therefore as $k_{21} - k_1$ becomes very small, the equation S6 becomes the equation typically used to convert signals to concentrations (Equation 1).

Line 268 and line 246: two (slightly) different values for the ion-molecule reaction rates are given here. I would recommend to use the same value in the model and in equation 1.

The modeled forward ion rate constants were taken to be $k_c = 2 \times 10^{-9} \text{ cm}^3 \text{ s}^{-1}$. As discussed in the SI, assuming all ion rate constants are equal does introduce error into the model, but this error is insignificant in comparison to uncertainties of the measurement and evaporation rate constants used in the model. We have tested the model with $k_1 = 1.9 \times 10^{-9} \text{ cm}^3 \text{ s}^{-1}$ and the results were visually identical to those shown in Figure 5 and 6. Therefore, we prefer to use $k_c = 2 \times 10^{-9} \text{ cm}^3 \text{ s}^{-1}$ to keep the model notation simple.

Line 293: please provide the value of the rate constant k_{21} here; this should be done for all rates by including their values in parentheses

We have added the collision rate constant value.

“The rate constant, k_{21} , is the collisional rate constant of $2 \times 10^{-9} \text{ cm}^3 \text{ s}^{-1}$.”

Line 329: “efficiently” instead of “inefficiently”?

Fixed.

Figure 7: The figure caption states a value of $4 \times 10^9 \text{ cm}^{-3}$ for the initial sulfuric acid concentration. However, in the legends different values for $[A1]$ are given. Are these the concentrations after the 3 s reaction time? If so, please mention this in the figure caption.

The reviewer is correct. We have added this clarification into the caption of the figures.

“Figure 6 Measured **sulfuric acid dimer to monomer signal ratio** (S_{195}/S_{160}) as a function of t_{CI} for DMA (a), EDA (b), and TMEDA (c) measured by nitrate CI at $[A_1]_0 \sim 4 \times 10^9 \text{ cm}^{-3}$. The tables in panels a-c provide the measured $[A_1]$ at that $[B]$ after **the 3 s acid-base reaction time**. Observations were fitted according to Equation 2 with the y-intercept shown by the dashed line. Panels d-f present modelled results for each base.

“Figure 7 Measured **sulfuric acid dimer to monomer signal ratios** (S_{195}/S_{160} for nitrate or S_{97} for acetate) as a function of CI reaction time using nitrate (a) and acetate CI (c). In both cases, $[A_1]_0$ was held constant at $4 \times 10^9 \text{ cm}^{-3}$. Panel (b) shows the modeled results for Put. **The table inside panel (a) and (c) provide the measured $[A_1]$ after the 3 s acid-base reaction time.**”

Line 374: Do these evaporation rates refer to the evaporation of DMA or A?

These are DMA evaporation rates.

“CI of N_3 leads to ions such as (i) $A_3^- \bullet \text{DMA}_3$ which evaporate at a rate of 10^4 s^{-1} into $A_3^- \bullet \text{DMA}_2$ and (ii) $A_3^- \bullet \text{DMA}_2$ and $A_3^- \bullet \text{DMA}$ which have predicted **DMA** evaporation rates of $\sim 10^{-1}$ and 10^{-2} s^{-1} ”

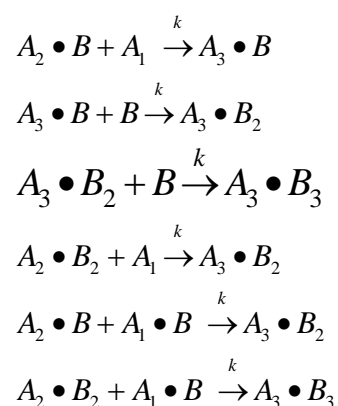
Line 425: better use “sources of dimer ions” than “dimer ion sources”

Agreed—much better phrasing.

“These reactions have little effect on the modeled dimer results since they introduce minor **sources of dimer ions**.”

Table 3: for the neutral pathway it seems the reaction $A_3B_2 + B$ is missing

This pathway is indeed included in our model. We added this missing reaction in Table 3 and Table S2.



Line 466: do you mean “low” instead of “high”?

We do mean high. Since the $[\text{DMA}]$ is much lower than $[A_1]$, we do not anticipate seeing $[A_5 \bullet \text{DMA}_5]$ as high as 10^7 cm^{-3} . We expect to see pentamers with less than 5 DMA, closer to 3 or even 4.

References: please use same style for all references, i.e. remove hyperlinks and add page numbers for all references, etc.

We have standardized the references to follow ACP guidelines. Unfortunately, Endnote does not track changes so it is difficult to show the changes in the manuscript.

SI, Line 39: “cm-3” instead of “cm3 ”, also better to use “s-1” instead of “Hz”

Thanks for catching that typo. However, we would prefer to use Hz cm^{-3} as Hz better implies signal of the MS, and this would keep our measurements consistent with the sensitivity curves Zhao et al. (2010) reported.

SI, Equation S6: see comment above

See response above.

Table S1: In a previous paper by the same authors (Jen et al., 2016, GRL) it was concluded that diamines are a more potent source of new particles in comparison with DMA. However, from the evaporation rates listed in Table 1 this conclusion does not seem to be supported due to the rather high evaporation rates E1 for the diamines (50 times higher than for DMA) and the crucial role of A1B1 in terms of cluster formation. How can this discrepancy be explained and how does it affect the conclusions from the present paper?

The evaporation rates listed in Table S1 are not the true evaporation rates for two reasons:

- 1) These are just evaporation rates used in our modeling. The model is not perfect as it assumes certain pathways for cluster formation to reduce the number of fitted parameters. A more comprehensive model (like ACDC) is needed to capture all possible pathways.
- 2) Even with our assumed model, these evaporation rates imply that the cluster lifetimes are on the order of the 3 s acid-base neutral reaction time. Our experiment does not have the time sensitivity to distinguish between clusters with lifetimes differing by a few seconds.

Regardless of the very large uncertainty in these evaporation rates, consideration must also be given to the evaporation rates for the larger clusters. The formation of $A_1 \cdot B_1$ is very crucial but assuming the evaporation of $A_1 \cdot B_1$ is the bottleneck to nucleation ($E_{2,3}=0 \text{ s}^{-1}$) will fail to distinguish the differences between DMA and the diamines. Two DMA molecules are needed to form a cluster without appreciable evaporation rates whereas just one diamine molecule is needed. This is key conclusion of Jen et al. (2016) and is further confirmed by computational results from Elm et al. (2016). There is no discrepancy between Jen et al. (2016) and this paper. In fact, they both tell the same story. The formation of $A_1 \cdot \text{Diamine}$ is likely the bottleneck to nucleation for these clusters whereas there are multiple bottlenecks to nucleation for sulfuric+DMA clusters.

We have mentioned both the large uncertainty of the evaporation rates and how this study relates to Jen et al. (2016) in the manuscript and SI. Though the reviewer brings up a subtle and very important point, we have decided to not add any more lines to the paper.

Reviewer #2

This paper reports interesting experimental work on the behaviour of atmospherically relevant cluster upon charging and subsequent travel through mass spectrometric instruments. The data has been analysed with a modelling scheme, and result help to understand state of the art instruments in the field of atmospheric particle formation as well as the formation process itself.

On top of the issues raised by the other two anonymous referees, I have only a few minor points that the authors could consider clarifying:

Lines 32 & 46: "...its clusters react with other trace compounds to produce stable electrically neutral ..." Is the idea here that the clusters are formed of sulphuric acid and water only, and the other compounds are added in the reactions mentioned? This could be specified, as now speaking of clusters existing before the reactions with trace compounds sound a bit confusing

The intent of that sentence is to say that sulfuric acid and cluster containing sulfuric acid (which could also contain water, ammonia, etc.) react with trace gases to form stable, electrically neutral clusters. We have clarified our meaning in these two lines (references removed to make it easier to read).

“In the atmospheric boundary layer, sulfuric acid often participates in nucleation **by reacting** with other trace compounds to produce stable, electrically neutral molecular clusters”

“The first process, neutral cluster formation, follows a sequence of acid-base reactions whereby sulfuric acid vapor and its **subsequent** clusters react with basic molecules to produce clusters that are more stable than aqueous sulfuric acid clusters.”

Line 55 Maybe add "that of" in the sentence "... proton affinity than THAT OF acetate..."

Agreed.

Line 236 Might be better to change "Following the neutral reactions . . ." -> "Following the neutral clustering reactions—"

Agreed.

Lines 343-348: “For all three diamines, we were unable to reproduce the observations with other combinations of reactions and evaporation rates. The model only matched ~ the observed trends when turning off the CI or formation of A2*diamine2.

Other explanations may exist to explain the differences between DMA and diamines observations (the most likely being semi-efficient [NITRATE?] CI of A2*diamine instead of zero nitrate CI of A2*diamine2), but additional thermochemical data (e.g., from more targeted experiments and computational chemistry) are needed to better inform the model.
“

The explanation above feels slightly confusing as it seems that first it is stated that no other choice would lead to the observed trends, but then later another possibility is suggested. Could this be clarified? And could the word nitrate be added where I have inserted it in brackets in the above text?

Yes, it is a bit confusing. We have reworded this section.

“For all three diamines, we were unable to reproduce the observations with other combinations of reactions and evaporation rates. The model only matched the observed trends by turning off the CI or formation of $A_2\bullet\text{diamine}_2$.

However, several of the modeled reactions are simplified versions of multi-step reactions. For example, preventing the formation of $A_2\bullet\text{TMEDA}_2$ could also mean $A_2\bullet\text{TMEDA}_2$ forms at the collision rate but instantly decomposes into $A_2\bullet\text{TMEDA}$. Furthermore, differences between DMA and diamine observations could instead be explained by semi-efficient nitrate CI of $A_2\bullet\text{diamine}$ because the existence of high $[A_2\bullet\text{diamine}_2]$ is unlikely due to its high basicity. Preventing $A_2\bullet\text{diamine}_2$ from forming and semi-efficient CI of $A_2\bullet\text{diamine}$ could lead to identical results as shown in the model for EDA and TMEDA. Additional thermochemical data (e.g., from more targeted experiments and computational chemistry) are needed to better inform the model. Regardless, our observations and modeling show that dimer’s neutral formation pathways and/or the nitrate CI differs between the DMA and diamine systems.”

Reviewer #3

Review of Jen et al., Chemical ionization of clusters formed from sulfuric acid and dimethylamine or diamines

Summary and General Comments: The authors present a series of experiments designed to assess the utility of nitrate ion CIMS techniques for the detection of H_2SO_4 - base clusters that lead to the formation of new particles in the atmosphere. Nitrate ion CIMS has been used for detection of low vapor pressure trace gases previously, and is well known to be a highly sensitive, but very specific reagent ion. The authors extend this logic to the detection of clusters, under the premise that nitrate ions may be selection in ionization of neutral (or less acidic) clusters. To demonstrate the effect, they contrast the nitrate CIMS technique with acetate CIMS techniques, demonstrating that nitrate ion chemistry does not ionize all of the clusters generated in the flow reactor. The authors combine both experiment and simple models to describe the results.

The manuscript is well written, and should be accepted following the authors attention to the following minor comments:

Specific Comments: I was surprised there was not a reference to the use of acetate ions for gasphase acid measurements (e.g., Veres et al. 2008 (Int. J. Mass Spectrom., doi:10.1016/j.ijms.2008.04.032, 2008)

Veres et al. is indeed the seminal paper presenting the use of acetate to chemically ionize gas phase acids. We should note that Veres et al. differs from this study in that we are chemically

ionizing with acetate at atmospheric pressure. We have added the reference to illustrate the differences of proton affinities for acetate compared to nitrate.

“Acetate CI has been used previously to detected organic acids less acidic than sulfuric acid in the atmosphere, providing evidence that its higher proton affinity could chemically ionize more basic clusters (Veres et al., 2008). Subsequently, Jen et al. (2015) showed that CI with $(\text{HNO}_3)_{1-2} \cdot \text{NO}_3^-$ leads to significantly lower neutral concentrations of clusters with 3 or more sulfuric acid molecules and varying numbers of DMA molecules compared to results using acetate reagent ions.”

I found the notations S160 / S125 (and similar) that are used throughout the figures to be confusing to the non-expert. I suggest defining these relationships in each figure caption. For example in Fig. 5, “Measured and modeled sulfuric acid-to-nitrate ion ratio (S160 / S125)” This helps keep the reader engaged and not flipping back to the definition in the manuscript. The same is true for S195 / S160 or S160 / S97.

We agree that this notation can be confusing to those not familiar with the masses of the clusters (which is the vast majority of the readers). We have taken the advice of the reviewer and added those clarifying remarks.

“Figure 5 Measured (a,b) and modeled (c, d) sulfuric acid monomer to nitrate signal ratio (S_{160}/S_{125}) as a function of CI reaction time for DMA (a, c) and EDA (b, d). The measurements were conducted with nitrate as the reagent ion and at $[A_1]_0 \sim 4 \times 10^9 \text{ cm}^{-3}$. Each color represents a different [B] with the linear regressions for the measurements given in colored text.”

“Figure 6 Measured sulfuric acid dimer to monomer signal ratio (S_{195}/S_{160}) as a function of t_{CI} for DMA (a), EDA (b), and TMEDA (c) measured by nitrate CI at $[A_1]_0 \sim 4 \times 10^9 \text{ cm}^{-3}$. The tables in panels a-c provide the measured $[A_1]$ at that [B] after the 3 s acid-base reaction time. Observations were fitted according to Equation 2 with the y-intercept shown by the dashed line. Panels d-f present modelled results for each base. “

“Figure 7 Measured sulfuric acid dimer to monomer signal ratios (S_{195}/S_{160} for nitrate or S_{97} for acetate) as a function of CI reaction time using nitrate (a) and acetate CI (c). In both cases, $[A_1]_0$ was held constant at $4 \times 10^9 \text{ cm}^{-3}$. Panel (b) shows the modeled results for Put. The table inside panel (a) and (c) provide the measured $[A_1]$ after the 3 s acid-base reaction time.”

“Figure 8 Measured bare sulfuric acid trimer to monomer signal ratio (S_{293}/S_{160}) as a function of t_{CI} for DMA (a), EDA (b), and TMEDA (c) detected by nitrate CI at $[A_1]_0 = 4 \times 10^9 \text{ cm}^{-3}$.”

“Figure 9 Nitrate measured signal ratio between $A_3 \cdot B$ and sulfuric acid monomer ($S_{A_3 \cdot B}/S_{160}$) as a function of t_{CI} for DMA (a), EDA (b), and TMEDA (c) at $[A_1]_0 = 4 \times 10^9 \text{ cm}^{-3}$.”

“Figure 10 Nitrate measured signal ratio between $A_4 \cdot B$ and sulfuric acid monomer ($S_{A_4 \cdot \text{diamine}}/S_{160}$) as a function of CI reaction time for EDA (a), Put (b), and TMEDA (c).”

Line 123-124: Are the reagent ion cluster distributions those observed in the mass spectrometer or those calculated to be in the source region. I would expect there to be a considerable difference between the reagent ions in the ion-molecule reaction region and

those detected by the mass spectrometer following collisional dissociation. How might the reagent ion cluster size impact its ability to undergo proton transfer?

The reagent ion distribution is measured by the Cluster CIMS. We believe the measured distribution does reflect the makeup in the ion-molecule reaction region as we tuned the Cluster CIMS to minimize cluster fragmentation. Measurements on nitrate cluster binding enthalpies supports our observations for the nitrate ion distribution, with dimer ion being the most strongly bonded and thus the highest in signal/concentration (Lovejoy and Bianco, 2000). In addition, the Cluster CIMS does not have a specific collisional dissociation chamber (CDC) like most CIMS instruments; instead it only has conical octopoles to focus the ion clusters prior to the quadrupole. With that being said, we are still uncertain on the exact composition of the reagent ion clusters, i.e. what else is attached to the nitrate clusters. Tanner and Eisele (1995) showed RH does not affect nitrate dimer chemical ionization of sulfuric acid. At high base concentrations and low sulfuric acid concentrations, base molecules cluster with the reagent ions, as shown in Simon et al. (2016). It still is not known how base ligands on the reagent ions affect its chemical ionization abilities.

We have explicitly written out our assumption about treating the nitrate dimer and trimer (and all the acetate ions) as the essentially the same ion during CI. We do take into account mass dependent sensitivity which is explained in the SI.

“The **measured** reagent ions for nitrate CI was $(\text{HNO}_3)_{1-2} \cdot \text{NO}_3^-$, and the reagent ions for acetate CI were $\text{H}_2\text{O} \cdot \text{CH}_3\text{CO}_2^-$, $\text{CH}_3\text{CO}_2\text{H} \cdot \text{CH}_3\text{CO}_2^-$, and CH_3CO_2^- (in order of abundance). **The nitrate dimer and trimer are assumed to chemically ionize at equal rate constants, and the three acetate ions are assumed to chemically ionize in identical manners.**”

Line 126: What is the nominal cluster size used to calculate the assumed collision rate? Is there reason to suspect that the cluster size is different in nitrate and acetate mode?

The rate constant for the chemical ionization of sulfuric acid and nitrate dimer has been measured and is $1.9 \times 10^{-9} \text{ cm}^3 \text{ s}^{-1}$. The measured trimer rate constant is a bit slower at $1.7 \times 10^{-9} \text{ cm}^3 \text{ s}^{-1}$ but this number is uncertain due to ion decomposition at $T > 273 \text{ K}$ (Viggiano et al., 1997). To our knowledge, the dipole moments of acetate and its clusters has not been measured. Though acetate dimer and monomer are about the same mass as nitrate dimer and monomer, respectively, the dipole moments will have a larger influence on the collision rate than mass ($m^{1/2}$ vs. μ) (Su, 1973). Thus, we have assumed acetate and nitrate have similar collision rate constants with sulfuric acid. Such small differences between collision rate constants would not explain the very large differences between the cluster concentrations detected by nitrate and acetate.

References cited in this response:

- Elm, J. and Jen, C. N.: Strong Hydrogen Bonded Molecular Interactions between Atmospheric Diamines and Sulfuric Acid, *The Journal of Physical Chemistry A*, 120(20), 3693, doi:10.1021/acs.jpca.6b03192, 2016.
- Lovejoy, E. R. and Bianco, R.: Temperature Dependence of Cluster Ion Decomposition in a Quadrupole Ion Trap †, *The Journal of Physical Chemistry A*, 104(45), 10280, doi:10.1021/jp001216q, 2000.
- Simon, M., Heinritzi, M., Herzog, S., Leiminger, M., Bianchi, F., Praplan, A., Dommen, J., Curtius, J. and Kurten, A.: Detection of dimethylamine in the low pptv range using nitrate chemical ionization atmospheric pressure interface time-of-flight (CI-APi-TOF) mass spectrometry, *Atmospheric Measurement Techniques*, 9(5), 2135, doi:10.5194/amt-9-2135-2016, 2016.
- Su, T.: Theory of ion- polar molecule collisions. Comparison with experimental charge transfer reactions of rare gas ions to geometric isomers of difluorobenzene and dichloroethylene, *The Journal of Chemical Physics*, 58(7), 3027–3037, doi:doi:http://dx.doi.org/10.1063/1.1679615, 1973.
- Tanner, D. J. and Eisele, F. L.: Present OH measurement limits and associated uncertainties, *Journal of Geophysical Research*, 100(D2), 2883, doi:10.1029/94jd02609, 1995.
- Viggiano, A. A., Seeley, J. V. and Mundis, P. L.: Rate Constants for the Reactions of $\text{XO}_3\text{-(H}_2\text{O)}_n$ ($\text{X} = \text{C, HC, and N}$) and $\text{NO}_3\text{-(HNO}_3\text{)}_n$ with H_2SO_4 :Implications for Atmospheric Detection of H_2SO_4 , *The Journal of ...*, 1997.
- Zhao, J., Eisele, F. L., Titcombe, M., Kuang, C. and McMurry, P. H.: Chemical ionization mass spectrometric measurements of atmospheric neutral clusters using the cluster-CIMS, *Journal of Geophysical Research*, 115(D8), doi:10.1029/2009jd012606, 2010.

Chemical ionization of clusters formed from sulfuric acid and dimethylamine or diamines

Coty N. Jen^{1,2*}, Jun Zhao^{1,3}, Peter H. McMurry¹, David R. Hanson⁴

¹Department of Mechanical Engineering, University of Minnesota – Twin Cities, 111 Church St. SE, Minneapolis, MN, 55455, USA

² now at Department of Environmental Science, Policy, and Management, University of California, Berkeley, Hilgard Hall, Berkeley, CA, 94720

³ now at Institute of Earth Climate and Environment System, Sun Yat-sen University, 135 West Xingang Road, Guangzhou 510275, China

⁴Department of Chemistry, Augsburg College, 2211 Riverside Ave., Minneapolis, MN, 55454, USA

*Correspondence to: Coty N. Jen (jenco@berkeley.edu)

Abstract: Chemical ionization (CI) mass spectrometers are used to study atmospheric nucleation by detecting clusters produced by reactions of sulfuric acid and various basic gases. These instruments typically use nitrate to deprotonate and thus chemically ionize the clusters. In this study, we compare cluster concentrations measured using either nitrate or acetate. Clusters were formed in a flow reactor from vapors of sulfuric acid and dimethylamine, ethylene diamine, tetramethylethylene diamine, or butanediamine (also known as putrescine). These comparisons show that nitrate is unable to chemically ionize clusters with high base content. In addition, we vary the ion-molecule reaction time to probe ion processes which include proton-transfer, ion-molecule clustering, and decomposition of ions. Ion decomposition upon deprotonation by acetate/nitrate was observed. More studies are needed to quantify to what extent ion decomposition affects observed cluster content and concentrations, especially those chemically ionized with acetate since it deprotonates more types of clusters than nitrate.

Model calculations of the neutral and ion cluster formation pathways are also presented to better identify the cluster types that are not efficiently deprotonated by nitrate. Comparison of model and measured clusters indicate that sulfuric acid dimer with two diamines and sulfuric acid trimer with two or more base molecules are not efficiently chemical ionized by nitrate. We conclude that acetate CI provides better information on cluster abundancies and their base content than nitrate CI.

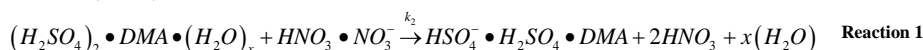
Introduction:

Atmospheric nucleation is an important source of global atmospheric particles (IPCC, 2014). In the atmospheric boundary layer, sulfuric acid often participates in nucleation (Weber et al., 1996; Kuang et al., 2008; Kulmala et al., 2004; Riipinen et al., 2007) and its clusters by reacting with other trace compounds to produce stable, electrically neutral molecular clusters; these compounds include ammonia (Kirkby et al., 2011; Coffman and Hegg, 1995; Ball et al., 1999), amines (Almeida et al., 2013; Zhao et al., 2011; Glasoe et al., 2015), water (Leopold, 2011), and oxidized organics (Schobesberger et al., 2013). The primary instruments used for detecting freshly nucleated, sulfuric acid-containing clusters are atmospheric pressure chemical ionization mass spectrometers (CIMS) such as the Cluster CIMS (Zhao et al., 2010; Chen et al., 2012) and the CI atmospheric pressure interface-time of flight mass spectrometer (CI-API-ToF) (Jokinen et al., 2012). Both mass spectrometers use nitrate to chemically ionize neutral sulfuric acid clusters. Depending upon conditions, NO_3^- core ions generally have one or more HNO_3 and possibly several H_2O ligands. The signal ratio of the ion cluster to the reagent ion translates to the neutral cluster concentration (Berresheim et al., 2000; Hanson and Eisele, 2002; Eisele and Hanson, 2000).

The amounts and types of ions detected by the mass spectrometer are affected by four key processes: the abundance of neutral clusters, their ability to be chemically ionized, product ion decomposition, and clustering reactions of the product ions (ion-induced clustering, IIC). The first process, neutral cluster formation, follows a sequence of acid-base reactions (Chen et al., 2012; Jen et al., 2014; Almeida et al., 2013; McGrath et al., 2012) whereby sulfuric acid vapor and its subsequent clusters react with basic molecules to produce clusters that are more stable than

aqueous sulfuric acid clusters. The concentration of a specific cluster type depends on its stability (i.e. evaporation rates of the neutral cluster) and the concentrations of precursor vapors (i.e. the formation rate).

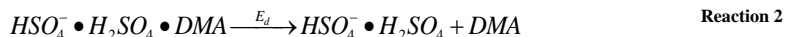
Neutral clusters then need to be ionized to be detected with a mass spectrometer. In most prior work, this has been accomplished by chemical ionization with the nitrate ion whereby the neutral clusters are exposed to nitrate for a set amount of time known as the chemical ionization reaction time (or ion-molecule reaction time). Chemical ionization (CI) can be conceptualized as another acid-base reaction where an acid (sulfuric acid) donates a proton to the basic reagent ion (nitrate, the conjugate base of nitric acid). To illustrate, the CI reaction of an aminated sulfuric acid dimer, $(H_2SO_4)_2 \cdot DMA$, is shown in [Reaction 1](#).



This dimer of sulfuric acid contains a dimethylamine (DMA) molecule and x water molecules. At room temperature, water molecules evaporate upon ionization or entering the vacuum region and are assumed to not significantly affect chemical ionization rates. The forward rate constant, k_2 , is assumed to be the collisional rate coefficient of $1.9 \times 10^{-9} \text{ cm}^3 \text{ s}^{-1}$ (Su and Bowers, 1973), while the reverse rate constant is zero.

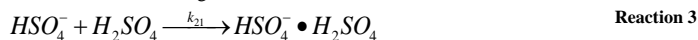
Reaction 1 can be extended to CI reactions for larger neutral clusters of sulfuric acid, with the assumption that every collision between nitrate and a sulfuric acid cluster results in an ionized cluster. However, Hanson and Eisele (2002) presented evidence that some clusters of sulfuric acid and ammonia were not amenable to ionization by $(HNO_3)_{1-2} \cdot NO_3^-$. [Acetate CI has been used previously to detect organic acids less acidic than sulfuric acid in the atmosphere, providing evidence that its higher proton affinity could chemically ionize more basic clusters \(Veres et al., 2008\).](#) Subsequently, ~~In addition,~~ Jen et al. (2015) showed that CI with $(HNO_3)_{1-2} \cdot NO_3^-$ leads to significantly lower neutral concentrations of clusters with 3 or more sulfuric acid molecules and varying numbers of DMA molecules compared to results using acetate reagent ions. Furthermore, neutral cluster concentrations detected using acetate CI are in overall better agreement with values measured using a diethylene glycol mobility particle sizer (DEG MPS). As no other experimental conditions changed except the CI reagent ion, we hypothesized that nitrate's lower proton affinity than [that of](#) acetate renders it less able to chemically ionize clusters that contain nearly equal amounts of sulfuric acid and base. Poor CI efficiency reduces the amount and types of ions detected by the mass spectrometer.

After neutral clusters are ionized, the resulting ion may decompose. Experimental studies have shown ion decomposition in the ammonia-sulfuric acid system at 275 K (Hanson and Eisele, 2002), and computational chemistry studies present evaporation rates of ion clusters of sulfuric acid with various bases on the order of the CI reaction time used here (Kurtén et al., 2011; Lovejoy and Curtius, 2001; Ortega et al., 2014). For example, these studies predict an evaporation rate, E_d (Reaction 2), of DMA from a sulfuric acid dimer ion with 1 DMA molecule of $\sim 100 \text{ s}^{-1}$ at 298 K (Ortega et al., 2014).



Experimental observations at room temperatures have never seen the aminated sulfuric acid dimer ion, even at CI reaction times as short as a few ms. Thus, the decomposition rate is likely even faster than the computed value of $\sim 100 \text{ s}^{-1}$ at 298 K (Ortega et al., 2014).

Ion clusters can also be produced by ion-induced clustering (IIC) whereby the bisulfate ion (HSO_4^-), formed by CI of sulfuric acid monomer, further reacts with H_2SO_4 (with ligands) and larger clusters. Charged clusters can also cluster with neutrals to form larger ion clusters. The signal due to these IIC products must be subtracted from the observed signals to determine neutral cluster concentrations. Specifically, the sulfuric dimer ion can be formed via the IIC pathway given in [Reaction 3](#), with ligands not shown.



The forward rate constant, k_{21} , is the collisional rate constant of $2 \times 10^{-9} \text{ cm}^3 \text{ s}^{-1}$ because this reaction involves switching ligands between the two clusters. Both reactants also contain water, nitrate, and/or base ligands that detach during

measurement. IIC-produced dimer signal interferes with the CI detected neutral dimer but can be calculated from measured sulfuric acid vapor concentrations and CI reaction times (Chen et al., 2012; Hanson and Eisele, 2002).

IIC can also produce larger clusters, but in general its contribution is less than for the dimer, even if all rates are assumed to be collisional. Furthermore, bisulfate may not efficiently cluster with chemically neutralized sulfate salt clusters formed by reactions of sulfuric acid and basic compounds. If so, assuming the collisional rate constant for all IIC-type reactions would lead to an over-correction of the neutral cluster concentrations.

Measured CIMS signals reflect the combined influences of all these processes, with each occurring on time scales that depend on the chemistry, experimental parameters, and techniques. Assuming a process is either dominant or negligible can lead to large errors in reported neutral cluster compositions and concentrations. Here, neutral cluster formation, chemical ionization, IIC, and ion decomposition are examined experimentally and theoretically to determine the influence of each process on the abundance of ion clusters composed of sulfuric acid and various bases. These bases include DMA, ethylene diamine (EDA), trimethylethylene diamine (TMEDA), and butanediamine (also known as putrescine, Put). The diamines, recently implicated in atmospheric nucleation, react with sulfuric acid vapors to very effectively produce particles compared to monoamines (Jen et al., 2016). We present observations that 1) show a clear difference between acetate and nitrate CI for all clusters larger than the sulfuric acid dimer with any of the bases, 2) provide evidence of ion decomposition, and (3) identify specific bases that influence the detectability of the dimer neutral clusters. Also presented are modeling results that help elucidate specific processes that influence measurement: neutral cluster formation pathways, cluster types that do not undergo nitrate CI, and clusters that are formed by IIC.

Method:

Sulfuric acid clusters containing either DMA, EDA, TMEDA, or Put were produced in a flow reactor that allows for highly repeatable observations (see Jen et al. (2014) and Glasoe et al. (2015)). Glasoe et al. (2015) showed that the system has a high cleanliness level: 1 ppqv level or below for amines. Each amine was injected into the flow reactor at a point to yield ~3 s reaction time between the amine and sulfuric acid (see Jen et al. (2014) for a schematic). The initial sulfuric acid concentration ($[A_1]_0$) before reaction with basic gas was controlled at specified concentrations. The base concentration, $[B]$, was measured by the Cluster CIMS in positive ion mode (see SI of Jen et al. (2014) for further details) and confirmed with calculated concentrations (Zollner et al., 2012; Freshour et al., 2014). The dilute amines were produced by passing clean nitrogen gas over either a permeation tube (for DMA and EDA) or a liquid reservoir (TMEDA and Put), and further diluted in a process described in Zollner et al. (2012). The temperature of the flow reactor was held constant throughout an experiment but varied day-to-day from 296-303 K to match room temperature. This was done to minimize thermal convection which induces swirling near the Cluster CIMS sampling region. The relative humidity was maintained at ~30%, and measurements were done at ambient pressure (~0.97 atm). Total reactor N_2 flow rate was 4.0 L/min at standard conditions of 273 K and 1 atm.

Two types of experiments were conducted: one set where specific base, base concentration ($[B]$), and $[A_1]_0$ were varied at constant CI reaction time (similar to those in in Jen et al. (2014)), and the second set where CI reaction time was varied for a subset of reactant conditions (see Hanson and Eisele (2002) and Zhao et al. (2010)). The resulting concentrations were measured with the Cluster CIMS using either nitrate or acetate as the CI reagent ion. Nitrate and acetate were produced either by passing nitric acid or acetic anhydride vapor over Po-210 sources. Separate Po-210 sources and gas lines were used for the acetate and nitrate to avoid cross-contamination. The measured reagent ions for nitrate CI was $(HNO_3)_{1-2} \cdot NO_3^-$, and the reagent ions for acetate CI were $H_2O \cdot CH_3CO_2^-$, $CH_3CO_2H \cdot CH_3CO_2^-$, and $CH_3CO_2^-$ (in order of abundance). The nitrate dimer and trimer are assumed to chemically ionize at equal rate constants, and the three acetate ions are assumed to chemically ionize in identical manners. The inferred neutral cluster concentrations were calculated from the CI reaction time, measured and extrapolated mass-dependent sensitivity (see Supporting Information), and the assumed collisional rate constant between CI ion and sulfuric acid clusters (see Jen et al. (2014) and (2015) for a discussion on the data inversion process). The CI reaction time, t_{CI} , was determined from the inlet dimensions and electric field strength inside the sampling region; for this set of experiments, t_{CI} was fixed at 18 ms for nitrate and 15 ms for acetate.

Varying t_{CI} at fixed $[B]$ and $[A]_0$ was achieved by changing the electric field used to draw ions across the sample flow into the inlet. Similar experiments have been performed with other atmospheric pressure, CI mass spectrometer inlets (Hanson and Eisele, 2002;Zhao et al., 2010;Chen et al., 2012) with the detailed mathematical relationship between t_{CI} and ion signal ratios developed more in depth in the following sections and the SI.

Acetate vs. Nitrate Comparison:

Figure 1 (a and c) compare inferred cluster concentrations derived from measured signals (assuming the collisional rate constant, k_c , and no ion breakup) using acetate (red squares) and nitrate (black triangles) reagent ions at a constant $[A]_0 \sim 4 \times 10^9 \text{ cm}^{-3}$ for two different $[DMA]$. The grouped points represent clusters that contain equivalent number of sulfuric acid molecules (N_1 is the monomer, N_2 is the dimer, etc.) but with different number of DMA molecules (e.g., $A_4 \cdot DMA_{0-3}$ where A is sulfuric acid). The number of base molecules in each cluster is given by the grouping bracket. Since the tetramers and pentamers have similar mass ranges, N_4 clusters are given as half-filled symbols and N_5 clusters as outlined symbols. Note, N_1 is detected at different masses between the two reagent ions, with nitrate at $160 \text{ amu} = HSO_4 \cdot HNO_3$ and acetate at $97 \text{ amu} = HSO_4^-$. The total cluster concentrations, $[N_m]$, compared between the two CI ions are shown in Figure 1 (b and d). The notation used here differs slightly from Jen et al. (2014) such that $[N_m]$ denotes the total concentration for clusters that contain m sulfuric acids molecules (i.e., $[N_m] = [A_m] + [A_m \cdot B_1] + [A_m \cdot B_2] \dots$) and $A_m \cdot B_j$ represents a specific cluster type with m sulfuric acid molecules and j basic molecules (B). The measured $[N_1]$ and $[N_2]$ obtained using nitrate and acetate are in good agreement for DMA. In the set of bases studied in Jen et al. (2014) (ammonia, methylamine, DMA, and trimethylamine), DMA is the strongest clustering agent, and these results reaffirm the accuracy of previously reported values of $[N_1]$ and $[N_2]$ in Jen (2014) at high $[A]_0$.

Figures 2, 3, and 4 show the acetate and nitrate comparison for EDA, TMEDA, and Put, respectively. Although nitrate appears to consistently detect less $[N_1]$ than with acetate, the estimated systematic uncertainty on acetate detected $[N_1]$ is higher than with nitrate due to higher background signals detected by acetate, sensitivity for the low masses (see SI), and possible influence of diamines on the ion throughput in the mass spectrometer. Other factors that may influence the detected $[N_1]$ are discussed in the SI. The true acetate $[N_1]$ could be up to a factor of 5 lower. Therefore, for monomer clusters formed from diamines, it is difficult to conclude that acetate and nitrate lead to significant differences in measured $[N_1]$.

Unlike the other bases, Put was observed in the monomer using either nitrate or acetate CI (Figure 4). The presence of $A_4 \cdot \text{Put}$ indicates its binding energy must be higher than monomers containing the other bases. However, this ion still decomposes in roughly the $t_{CI} = 15 \text{ ms}$ as it is $\sim 0.1\%$ of $[N_4]$. Elm et al. (2016) has shown that the binding energy of $A_4 \cdot \text{EDA}$ is -11.1 kcal/mol and $A_4 \cdot \text{Put}$ is -15.4 kcal/mol , with $A_4 \cdot \text{DMA}$ closely matching $A_4 \cdot \text{EDA}$ at -11.38 kcal/mol (Nadykto et al., 2014; Bork et al., 2014). The higher neutral binding energies of $A_4 \cdot \text{Put}$ may translate to stronger ion binding energies than the other aminated monomers, though more studies are needed to confirm this.

Both acetate and nitrate primarily detect the bare dimer, with $[N_2]$ up to a factor of 5 higher with acetate CI than nitrate. The systematic uncertainties of the acetate measurement are due to similar reasons as those for $[N_1]$ and could lead to a factor of 2-3 times lower $[N_2]$ than reported here, are about a factor of 2-3 for similar reasons to the uncertainties for N_1 . These comparisons seem to suggest that for clusters formed from diamines, nitrate does not detect as many types of N_2 as does acetate; however, the large uncertainty in acetate $[N_2]$ prevents a definitive conclusion as to whether or not nitrate chemically ionizes all types of dimers. More information is gained from experiments that vary t_{CI} as they are more sensitive to the various formation pathways. These results are presented in the subsequent sections.

Figures 1 through 4 (b and d) clearly show that more of the larger clusters (N_3 and higher) were detected by acetate CI than nitrate. For all bases, the measured $[N_3]$ by acetate is up to a factor of 2 to 100 times higher than concentrations measured by nitrate CI. Nitrate detected small amounts of N_4 and no N_5 , likely due to the ionizable fraction of $[N_4]$ and $[N_5]$ falling below detection limits ($< 10^5 \text{ cm}^{-3}$). In addition as $[B]$ increases, the differences

Formatted: Subscript

Formatted: Superscript

Formatted: Font: Italic

Formatted: Font: Italic, Subscript

Formatted: Subscript

Formatted: Subscript

Formatted: Subscript

Formatted: Subscript

Formatted: Subscript

Formatted: Subscript

between acetate and nitrate cluster concentrations become more pronounced. This likely occurs because sulfuric acid clusters become more chemically neutral as $[B]$ increases, thereby decreasing their tendencies to donate protons to nitrate ions. The differences between acetate and nitrate measured cluster concentrations cannot be explained only by the larger uncertainties in the acetate measurements. The systematic uncertainties in acetate detected larger clusters is at most a factor of 2 below reported concentrations. Thus, acetate is more efficient than nitrate at chemically ionizing the larger cluster population.

The large differences between nitrate and acetate measured $[N_3]$ and $[N_4]$ provide information to better understand recent atmospheric and chamber measurements. Chen et al. (2012) and Jiang et al. (2011) published $[N_3]$ and $[N_4]$ measured in the atmosphere using a larger version of the Cluster CIMS (Zhao et al., 2010). For both studies, the measurements were conducted using nitrate CI and only at the clusters' bare masses (A_3 and A_4). Trimer and tetramer may have been under-detected, though this is uncertain because the atmosphere contains numerous compounds that may behave differently than DMA and diamines. If the actual concentrations of trimer and tetramer were higher than those reported by Jiang et al. (2011), then the fitted evaporation rate of $E_3=0.4\pm0.3\text{ s}^{-1}$ from Chen et al. (2012) is too high and the true value would be closer to 0 s^{-1} (collision-controlled or kinetic limit) that was reported by Kürten et al. (2014) at 278 K. In addition, Kürten et al. measured $[N_3]$ and $[N_4]$ about a factor of 10 lower than the collision-controlled limit. They attribute this discrepancy to decreased sensitivity for the larger ions, but it could also be due to inefficient CI by nitrate.

Comparing our results to the CLOUD experiments, the amount of clusters detected via nitrate CI using the Cluster CIMS differ from those detected by nitrate using the CI-API-ToF (Kürten et al., 2014). They observed more ion clusters that contained nearly equal number of sulfuric acid and DMA molecules (e.g., $A_3\cdot\text{DMA}_2$). Our experiments suggest that such highly neutralized clusters are not efficiently ionized by our nitrate core ions. We do not fully understand this difference but longer acid-base reaction times, the amount of ligands on the nitrate core ions, various inlet designs (e.g., corona discharge vs. our Po-210 or high vs. our low flow rates), temperature (278 K compared to our 300 K), and ion breakup upon sampling may all play a role.

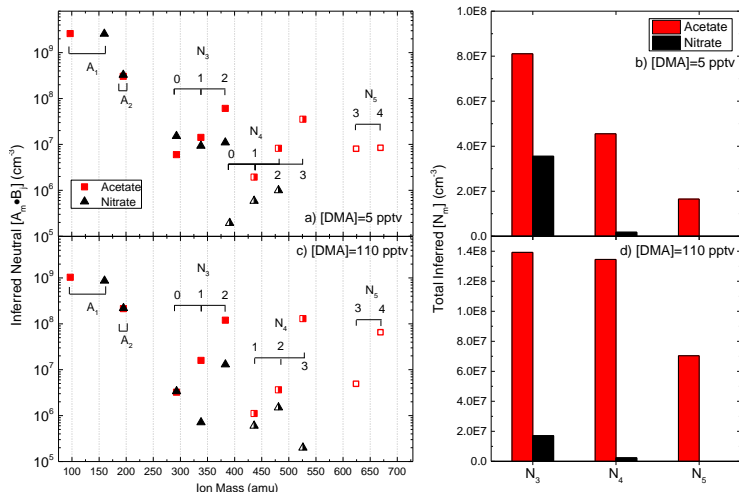
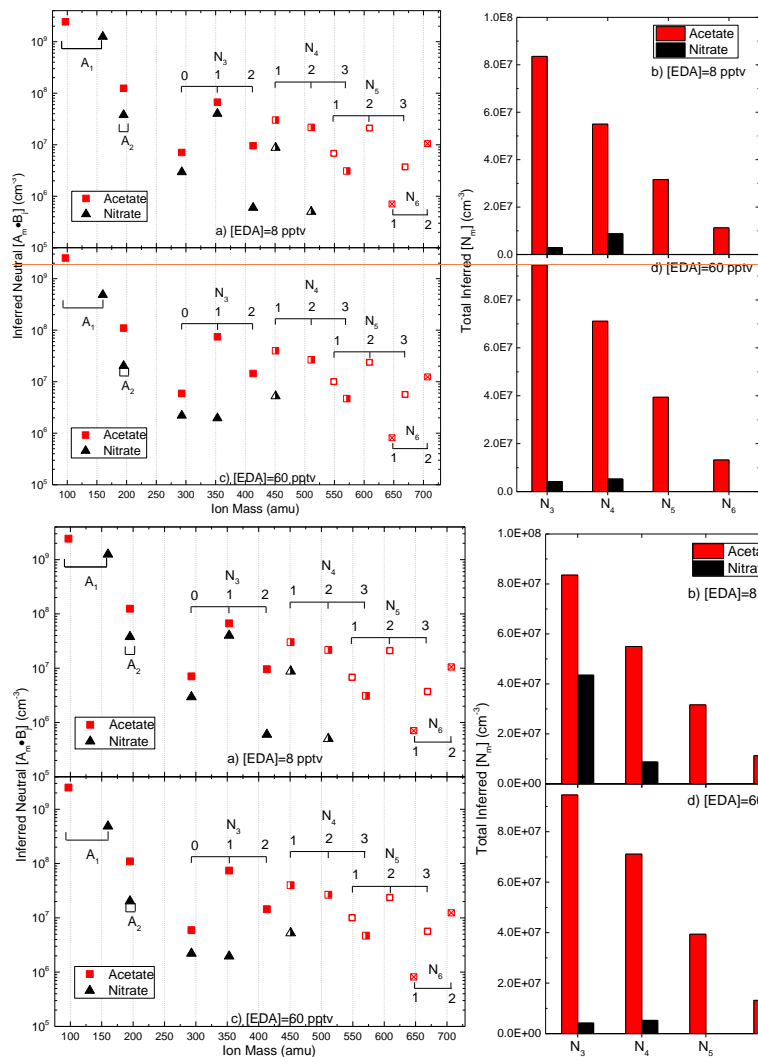


Figure 1 (a and c) Comparison of specific cluster concentrations ($[A_m \cdot B_j]$) using acetate (red squares) and nitrate (black triangles) reagent ions at two different $[DMA]$ and constant initial sulfuric acid concentration, $[A_1]_0 \sim 4 \times 10^9\text{ cm}^{-3}$. Each cluster species is shown at its ion mass. The brackets represent the number of DMA molecules in a cluster with a given number of sulfuric acid. The half-filled symbols show the tetramers and the outlined symbols are the pentamers. Bar graphs b and d compare total cluster concentration of a given size ($[N_m]$) between acetate (red) and nitrate (black) for the same $[DMA]$ and $[A_1]_0$ as a and b respectively.



Field Code Changed

Figure 2 (a and c) Comparison of specific cluster concentrations ($[A_m \cdot B_j]$) using acetate (red squares) and nitrate (black triangles) reagent ions at two different $[EDA]$ and constant initial sulfuric acid concentration, $[A_1]_0 \sim 4 \times 10^9 \text{ cm}^{-3}$. Each cluster species is shown at its ion mass. The brackets represent the number of EDA molecules in a cluster with a given number of sulfuric acid. The half-filled symbols show the tetramers, outlined symbols as the pentamers, and crossed symbols as 6-mer. Bar graphs b and d compare total cluster concentration of a given size ($[N_m]$) between acetate (red) and nitrate (black) for the same $[EDA]$ and $[A_1]_0$ as a and b respectively.

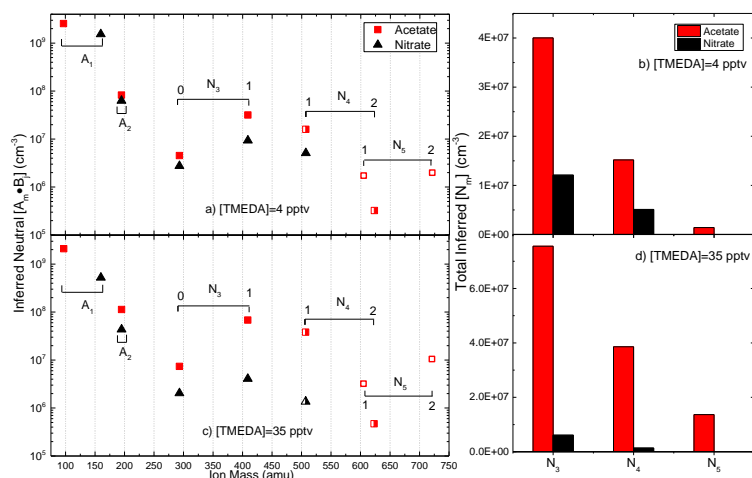


Figure 3 (a and c) Comparison of specific cluster concentrations ($[A_m \cdot B_j]$) using acetate (red squares) and nitrate (black triangles) reagent ions at two different [TMEDA] and constant initial sulfuric acid concentration, $[A_1]_0 \sim 4 \times 10^9 \text{ cm}^{-3}$. Each cluster species is shown at its ion mass. The brackets represent the number of TMEDA molecules in a cluster with a given number of sulfuric acid. The half-filled symbols show the tetramers and outlined symbols as the pentamers. Bar graphs b and d compare total cluster concentration of a given size ($[N_m]$) between acetate (red) and nitrate (black) for the same [TMEDA] and $[A_1]_0$ as a and b respectively.

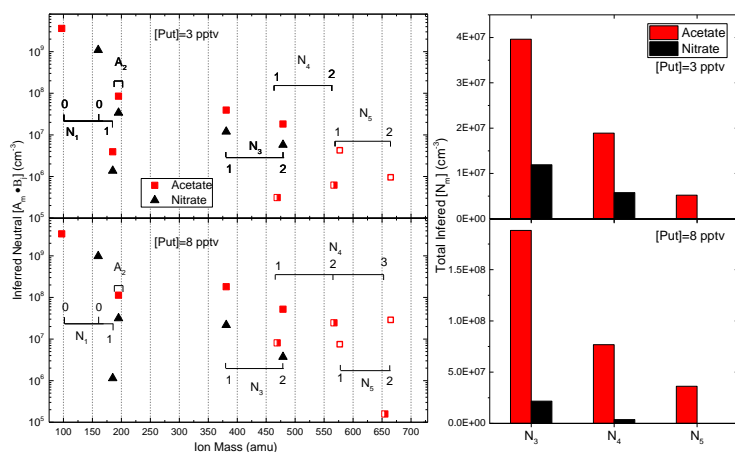


Figure 4 (a and c) Comparison of specific cluster concentrations ($[A_m \cdot B_j]$) using acetate (red squares) and nitrate (black triangles) reagent ions at two different [Put] and constant initial sulfuric acid concentration, $[A_1]_0 \sim 4 \times 10^9 \text{ cm}^{-3}$. Each cluster species is shown at its ion mass. The brackets represent the number of Put molecules in a cluster with a given number of sulfuric acid. The half-filled symbols show the tetramers and outlined symbols as the pentamers. Bar graphs b and d compare total cluster concentration of a given size ($[N_m]$) between acetate (red) and nitrate (black) for the same [Put] and $[A_1]_0$ as a and b respectively.

Chemical ionization efficiency clearly plays a role in both the types and amounts of clusters that can be detected. However, the concentrations in Figures 1 through 4 were calculated by assuming negligible contributions of

IIC and ion decomposition. The validity of these assumptions was tested by examining the ion behavior with CI reaction time (t_{CI}) for a variety of bases. Presented in the following sections are ion signal variations with t_{CI} and a discussion of possible scenarios that explain these observations. To help understand these measurements, we developed a model to describe these complex series of reactions that govern neutral cluster formation, chemical ionization, IIC, and ion decomposition. The model combines two box models: one for neutral cluster formation and one for the ion processes. When compared to observations, the model was useful in identifying the controlling process for the monomer and dimer but, due to the numerous reactions, only provided general scenarios to explain observations for the larger clusters.

Monomer, N_1 :

Over the 3 s neutral reaction time in this flow reactor (i.e., the reaction time between neutral sulfuric acid vapor and the basic gas), initial monomer concentration ($[N_1]$) is depleted as it forms larger clusters/particles and is lost to walls; N_1 may re-enter the gas phase by evaporation of larger clusters. Two types of N_1 may have significant abundances in the sulfuric acid and DMA system: A_1 and $A_1 \cdot \text{DMA}$. One computational chemistry study predicts the latter has an evaporation rate of 10^{-2} s^{-1} (all computed rates at 298 K unless otherwise stated) (Ortega et al., 2012) with others suggesting an evaporation rate closer to 10 s^{-1} (Nadykto et al., 2014; Bork et al., 2014).

Following the neutral clustering reactions, the remaining monomer is readily chemically ionized and the product ion can decompose and undergo IIC with the monomer or clusters. For example, the decomposition rate of $A_1 \cdot \text{DMA}$ is predicted to be 10^9 s^{-1} (Ortega et al., 2014). Therefore, whether or not $A_1 \cdot \text{DMA}$ is a significant fraction of the total monomer concentration, A_1^- is the only ion with significant abundance. This agrees with our experimental observations.

Neutral $[N_1]$ can be estimated from mass spectrometry signals because there is negligible ion breakup in the Cluster CIMS that leads to A_1^- . As discussed above, a number of experiments and the current results have shown this to be the case (Hanson and Eisele, 2002; Eisele and Hanson, 2000; Lovejoy and Bianco, 2000). The signal ratio of the sulfuric acid monomer at 160 amu for nitrate (S_{160}) to the nitrate ion at 125 amu (S_{125}) can be converted to neutral $[N_1]$ following Equation 1 (Eisele and Hanson, 2000), where t_{CI} is the CI reaction time.

$$\frac{S_{160}}{S_{125}} = k_1 [N_1] t_{CI} \quad \text{Equation 1}$$

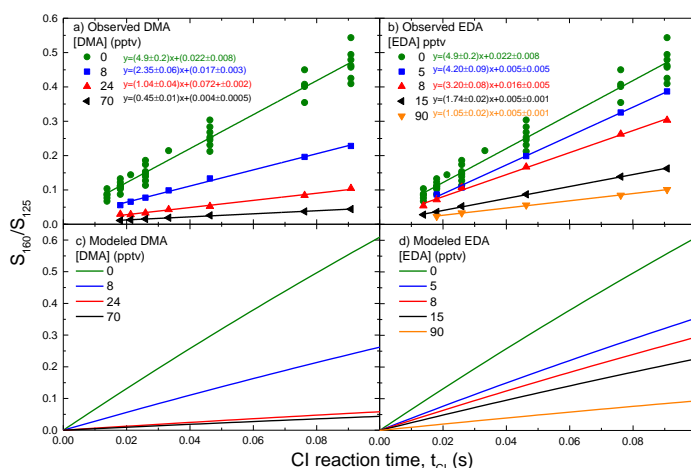
For $N_1 + \text{HNO}_3 \cdot \text{NO}_3^-$, $k_1 = 1.9 \times 10^{-9} \text{ cm}^3 \text{ s}^{-1}$ (Viggiano et al., 1997) which is assumed to not depend on whether water or bases are attached onto the monomer. Equation 1 was derived for short t_{CI} where reagent ion and neutral N_1 are not depleted. These assumptions are tenuous at long t_{CI} ; however, the rigorous analytical solution to the population balance equations (derived in the SI and given in Equation S6) shows that Equation 1 is a good approximation: at $t_{CI} = 15$ or 18 ms, the differences between Equation 1 and Equation S6 are $\sim 1\%$.

Figure 5 (a and b) shows the signal ratios as a function of t_{CI} for DMA and EDA as detected by nitrate CI at equivalent $[A_1]_0 = 4 \times 10^9 \text{ cm}^{-3}$. TMEDA and Put graphs look very similar to EDA (see SI). The green points shown in this figure and subsequent figures provide measurements at base concentration of 0 pptv from eight different days and offer a useful guide for the measurement uncertainty. For all base concentrations as t_{CI} increases, more $[N_1]$ is chemically ionized, leading to higher S_{160}/S_{125} . As $[B]$ increases, the signal ratios and therefore the slopes of the lines decrease. This indicates that $[N_1]$ is depleted during the 3 s neutral reaction time via uptake into large clusters that increase with $[B]$.

The model, as mentioned above, was used to interpret the results presented in Figure 5 and subsequent graphs. The neutral cluster concentrations after $[A_1]_0$ and $[B]$ react over the 3 s neutral reaction time are modeled first. This portion of the model also takes into account base dilution from its injection point in the flow reactor (see Jen et al.

274 (2014)), wall loss, and particle coagulation. However, the model does not take into account possible dilution of N_1 by
 275 the base addition flow which may affect measured $[N_1]$ as explained in the SI. The neutral model is then coupled to
 276 the ion model which simulates chemical ionization and IIC. Ion decomposition is implicitly included by assuming
 277 certain cluster types instantly decompose into the observed ion.

278 For the monomer, the model has identical neutral cluster formation pathways for all sulfuric acid and base
 279 systems. The acetate vs. nitrate comparison suggests that monomers containing various bases are chemically ionized
 280 similarly, with a slight possibility that nitrate may not chemically ionize sulfuric acid monomers that contain a diamine.
 281 The modeled reactions pertaining to the monomer are given in Table 1, where k_c is $2 \times 10^{-9} \text{ cm}^3 \text{ s}^{-1}$. The full list of
 282 modeled reactions, including loss of monomer to form larger clusters, is given in the SI.



283
 284 Figure 5 Measured (a,b) and modeled (c, d) sulfuric acid monomer to nitrate signal ratio (S_{160}/S_{125}) as a function of CI
 285 reaction time for DMA (a, c) and EDA (b, d). The measurements were conducted with nitrate as the reagent ion and at
 286 $[A_1]_0 \sim 4 \times 10^9 \text{ cm}^{-3}$. Each color represents a different $[B]$ with the linear regressions for the measurements given in colored
 287 text.

288 Table 1 Summary of possible pathways for neutral monomer formation and chemical ionization

Neutral formation	Nitrate CI and ion decomposition
<u>DMA and Diamines:</u> $A_1 + B \xrightleftharpoons[k_{-1}]{k} A \bullet B$	<u>DMA:</u> $A_1 + NO_3^- \xrightarrow{k_c} HNO_3 \bullet A_1^-$ $A_1 \bullet B + NO_3^- \xrightarrow{k_c} HNO_3 \bullet A_1^- \bullet B$ $HNO_3 \bullet A_1^- \bullet B \xrightarrow{fast} HNO_3 \bullet A_1^- + B$
	<u>Diamines:</u> $A_1 + NO_3^- \xrightarrow{k_c} HNO_3 \bullet A_1^-$ $A_1 \bullet B + NO_3^- \xrightarrow{?} HNO_3 \bullet A_1^- \bullet B$ $HNO_3 \bullet A_1^- \bullet B \rightarrow HNO_3 \bullet A_1^- + B$

Figure 5 (c and d) displays the modeled results for DMA and EDA at the same [B] and $[A_1]_0$ as the measurements presented in panels a and b. The model predicts the linear dependence of S_{160}/S_{125} on t_{CI} as seen in Equation 1. In addition, the predicted values of S_{160}/S_{125} and their dependence on [B] are in good qualitative agreement with observations. Including or excluding nitrate CI of $A_1 \bullet$ diamine has little effect on S_{160}/S_{125} because [B] is typically less than $[A_1]_0$ in these experiments. As a result, the majority of monomers will remain as A_1 even if the evaporation rate of the $A_1 \bullet B$ (E_1) is very small. Further experiments that quantify the fraction of $A_1 \bullet$ diamine in N_1 are needed to definitely conclude the efficacy of nitrate in chemically ionizing all N_1 .

Dimer, N_2 :

Neutral dimers (N_2) largely form by collision of the two types of monomers (A_1 and $A_1 \bullet B$) and, to a much lesser extent, decomposition of larger clusters. For sulfuric acid+DMA, the N_2 likely exists as $A_2 \bullet$ DMA and $A_2 \bullet$ DMA₂, with both clusters predicted to have low evaporation rates of $\sim 10^{-5} \text{ s}^{-1}$ (Ortega et al., 2012) with another study suggesting a higher evaporation rate of $A_2 \bullet$ DMA₂ $\sim 10^4$ times higher (Leverentz et al., 2013). Chemically ionizing these dimers results in ions that undergo IIC and ion decomposition. Computational chemistry predicts that $A_2 \bullet$ DMA₂ and $A_2 \bullet$ DMA have DMA evaporation rates of 10^8 s^{-1} and 10^2 s^{-1} , respectively (Ortega et al., 2014). However, the computed evaporation rate of $A_2 \bullet$ DMA may be too low because during the 18 ms CI reaction time used here, all N_2 are detected as A_2^- (195 amu). Similarly, the diamine molecule is lost from $A_2 \bullet$ diamine as all dimers were detected as A_2^- .

A_2^- can also be created from IIC between A_1^- and N_1 (see Reaction 2) that proceeds with a rate coefficient of k_{21} . Including both processes in the cluster balance equations leads to the ratio of sulfuric acid dimer (195 amu) to monomer (160 amu) signal intensities shown in Equation 2. This relationship includes a time-independent term (the $t_{CI}=0$ s intercept) that is proportional to the neutral dimer to monomer ratio in the sampled gas, and a term due to IIC that increases linearly with t_{CI} (Chen et al., 2012; Hanson and Eisele, 2002).

$$\frac{S_{195}}{S_{160}} = \frac{k_2}{k_1} \frac{[N_2]}{[N_1]} + \frac{1}{2} k_{21} [N_1] t_{CI} \quad \text{Equation 2}$$

The rate constants, k_{21} , are the collisional rate constant of $2 \times 10^{-9} \text{ cm}^3 \text{ s}^{-1}$. Equation 2 was also derived from the assumption of short t_{IC} . The relation for S_{195}/S_{160} vs. t_{CI} for long t_{CI} is also derived in the SI. Equation 2 is a good approximation for the more rigorous solution even at long t_{IC} .

Figure 6 (a-c) shows measured S_{195}/S_{160} as a function of t_{CI} for DMA, EDA, and TMEDA respectively as detected by nitrate CI at $[A_1]_0 = 4 \times 10^9 \text{ cm}^{-3}$. Put is similar to EDA and is presented in Figure 7 (left). For all bases, increasing the CI reaction time leads to more IIC-dimer. The observed linear increase in the S_{195}/S_{160} ratio for all bases provides evidence for the influence of IIC on dimer measurements (Equation 2). However, the y-intercepts for DMA exhibit a pattern that is distinctly different from those observed for the diamines, indicating different trends for the neutral monomer to dimer concentration ratios. For DMA, the y-intercept increases with increasing [B]. This is due to higher concentrations of base depleting the monomer and enhancing dimer concentrations. A different trend was observed for the diamines with the intercepts showing no clear dependence on diamine concentration.

Formatted: Superscript

Formatted: Superscript

Formatted: Superscript

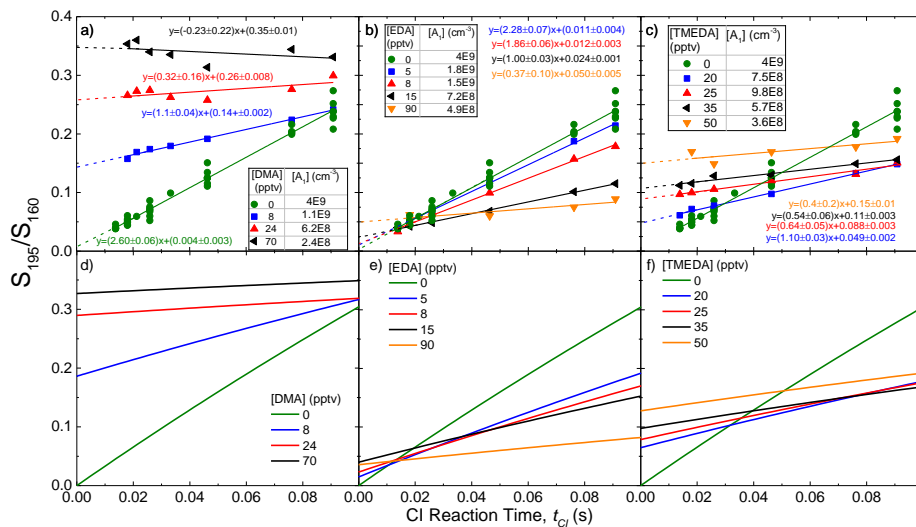


Figure 6 Measured sulfuric acid dimer to monomer signal ratio (S_{195}/S_{160}) as a function of t_{CI} for DMA (a), EDA (b), and TMEDA (c) measured by nitrate CI at $[A_1]_0 \sim 4 \times 10^9 \text{ cm}^{-3}$. The tables in panels a-c provide the measured $[A_1]$ at that $[B]$ after the 3 s acid-base reaction time. Observations were fitted according to Equation 2 with the y-intercept shown by the dashed line. Panels d-f present modelled results for each base.

There are a number of scenarios that could partly explain the diamine trends. First, the neutral trimer evaporation rate(s) could be very low such that the formation of trimer and larger clusters will deplete both $[N_2]$ and $[N_1]$. A_1 evaporation rate from $A_3 \cdot \text{DMA}$ is predicted to be $\sim 1 \text{ s}^{-1}$ (Ortega et al., 2012) and likely lower for cluster with diamines (Jen et al., 2016). The second possibility is A_2^+ could be the decomposition product of larger ions such as $A_3^+ \cdot \text{diamine}$ forming $A_2^+ + A_1 \cdot \text{diamine}$. A third possibility is that $A_2 \cdot \text{diamine}_2$ cannot be readily ionized by nitrate as compared to $A_2 \cdot \text{DMA}_2$ possibly due to differences in cluster configurations and dipole moments. As $[\text{diamine}]$ increases, the fraction of dimers containing two diamines increases, resulting in a growing fraction of N_2 that may not be ionizable by nitrate. For example, the model predicts $[A_2 \cdot \text{EDA}]$ is 10% of $[A_2 \cdot \text{EDA}_2]$ when $[\text{EDA}] = 90 \text{ pptv}$.

The dimer (S_{195}) to monomer signal (S_{97}) ratio for sulfuric acid+Put dimers measured using acetate CI as a function of t_{CI} was examined to better understand which of these explanations is the most relevant. As mentioned previously, acetate detects the sulfuric acid monomer as 97 amu, but the detected dimer is at 195 amu for both nitrate and acetate. Figure 7 shows the ratio of these signals for Put between nitrate (a) and acetate (c). At $[\text{Put}] = 40 \text{ pptv}$, acetate shows a S_{195}/S_{97} y-intercept 25 times higher than the intercepts shown in the nitrate graph. The higher y-intercepts are most likely due to improved CI efficiency. Decreased detection efficiency of 97 amu and an increased contribution due to $A_3^+ \cdot \text{diamine}$ decomposition due to better CI of N_3 by acetate may also contribute (although high $[A_3^+ \cdot \text{diamine}]$ in Figure 4 suggests these ions are stable enough during the acetate $t_{CI} = 15 \text{ ms}$). More acetate results similar to Figure 7 (c) are needed to draw a more definitive conclusion, but these comparisons do suggest that dimers containing 1-2 diamines are not inefficiently chemically ionized by nitrate in these experiments.

Formatted: Not Superscript/ Subscript

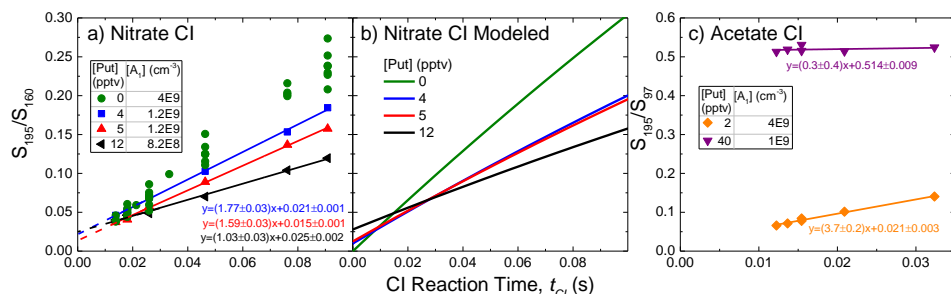


Figure 7 Measured dimer to monomer signal ratios (S_{195}/S_{160} for nitrate or S_{97} for acetate) as a function of CI reaction time using nitrate (a) and acetate CI (c). In both cases, $[A_1]_0$ was held constant at $4 \times 10^9 \text{ cm}^{-3}$. Panel (b) shows the modeled results for Put. The table inside panel (a) and (c) provide the measured $[A_1]$ after the 3 s acid-base reaction time.

The model adds more clarity on why N_2 containing diamines behave differently than DMA using nitrate CI. For DMA, the best fit to the observations was achieved by assuming all clusters can undergo nitrate ionization and can be formed by IIC. In addition, base evaporation rates from $A_2 \cdot B_2$ and sulfuric acid evaporation rates from the trimer were set to 0 s^{-1} ; increasing these evaporation rates (up to 10 and 5 s^{-1} respectively) had little effect on the ratio trends. The model also assumed that $A_3 \cdot B$ does not decompose into A_2 . Figure 6 (d) shows modeling results for DMA. To reproduce S_{195}/S_{160} trends of EDA and Put, the model followed that of DMA except $A_2 \cdot B_2$ cannot be ionized by nitrate. For TMEDA, the model also assumed $A_2 \cdot \text{TMEDA}_2$ does not form. Modeled results are shown in Figure 6 (e and f) for EDA and TMEDA, respectively, and Figure 7 (b) for Put. The modeled pathways for N_2 are listed in Table 2. Several of the modeled reactions are simplified versions of multi-step reactions. For example, preventing the formation of $A_2 \cdot \text{TMEDA}_2$ could also mean $A_2 \cdot \text{TMEDA}_2$ forms at the collision rate but instantly decomposes into $A_2 \cdot \text{TMEDA}$. For all three diamines, we were unable to reproduce the observations with other combinations of reactions and evaporation rates. The model only matched the observed trends when by turning off the CI or formation of $A_2 \cdot \text{diamine}_2$.

However, several of the modeled reactions are simplified versions of multi-step reactions. For example, preventing the formation of $A_2 \cdot \text{TMEDA}_2$ could also mean $A_2 \cdot \text{TMEDA}_2$ forms at the collision rate but instantly decomposes into $A_2 \cdot \text{TMEDA}$. Furthermore, other explanations may exist to explain the differences between DMA and diamines observations could instead be explained by the most likely being semi-efficient nitrate CI of $A_2 \cdot \text{diamine}$ because the existence of high instead of zero nitrate CI of $[A_2 \cdot \text{diamine}]_2$ is unlikely due to its high basicity. Preventing $A_2 \cdot \text{diamine}_2$ from forming and semi-efficient CI of $A_2 \cdot \text{diamine}$ could lead to identical results as shown in the model for EDA and TMEDA, but a Additional thermochemical data (e.g., from more targeted experiments and computational chemistry) are needed to better inform the model. Regardless, our observations and modeling show that dimer's neutral formation pathways and/or the nitrate CI differs between the DMA and diamine systems.

The model also provides an estimate of the fraction of $[A_2^-]$ formed by IIC at $t_{CI}=18 \text{ ms}$ (used for the nitrate CI experiments). For base concentration of 0 pptv, the model is very similar to what was measured in Figure 6, indicating that A_2^- is almost completely formed by $A_1^- + A_1$ (i.e., is an IIC artifact) and not by the CI of A_2 . The abundance of A_2 is low at 300 K (Hanson and Lovejoy, 2006), below detection limit of the Cluster CIM. For DMA, IIC dimers typically account for 1% (less at high [DMA]) of the total dimer signal which agrees with the conclusions drawn in Jen et al. (2015). In contrast, the IIC fraction of A_2^- using nitrate for EDA and Put is $\sim 50\%$, due to the potentially large fraction N_2 not undergoing chemical ionization. The nitrate ion's inability to chemically ionize some of the dimers is further highlighted since IIC is suppressed in the diamine system: less N_1 is available (due to formation of larger clusters) thus both $[A_1]$ and $[A_1^-]$ are depressed. IIC-produced A_2^- accounts for $\sim 20\%$ of the total dimer signal for TMEDA. However, these numbers are uncertain due to the assumptions in the model and uncertainties in the

Formatted: Subscript
Formatted: Subscript
Formatted: Subscript
Formatted: Subscript

measurement. For instance, the model is not sensitive to whether A_1^- can cluster with $A_1 \bullet B$, which would significantly influence the amount of IIC dimer without significantly affecting S_{195}/S_{160} . IIC contributes much less A_2^- when acetate is used as the reagent ion because acetate detects up to 5 times more total neutral dimer concentration ($[N_2]$) than nitrate when base is present. Acetate measurements show that IIC produced ~3% of the $[A_2^-]$ when $[Put]=2$ pptv and near zero when $[Put]=40$ pptv (Figure 7 c).

Table 2 Summary of possible pathways for neutral and ion dimer formation

Neutral formation	Nitrate CI and ion decomposition reactions	IIC reactions (only A_1^-)
DMA, Put, EDA: $A_1 \bullet B + A_1 \xrightarrow{k} A_2 \bullet B$ $A_1 \bullet B + A_1 \bullet B \xrightarrow{k} A_2 \bullet B_2$ $A_2 \bullet B + B \xrightarrow{k} A_2 \bullet B_2$ $A_2 \bullet B_2 \xrightarrow{E_{2B}} A_2 \bullet B + B$ TMEDA: $A_1 \bullet B + A_1 \xrightarrow{k} A_2 \bullet B$ $A_1 \bullet B + A_1 \bullet B \not\rightarrow A_2 \bullet B_2$ $A_2 \bullet B + B \not\rightarrow A_2 \bullet B_2$	DMA: $A_2 \bullet B + NO_3^- \xrightarrow{k_c} A_2^- \bullet B + HNO_3$ $A_2^- \bullet B \xrightarrow{fast} A_2^- + B$ $A_2 \bullet B_2 + NO_3^- \xrightarrow{k_c} A_2 \bullet B_2^- + HNO_3$ $A_2^- \bullet B_2 \xrightarrow{fast} A_2^- \bullet B$ Diamines: $A_2 \bullet B + NO_3^- \xrightarrow{k_c} A_2^- \bullet B$ $A_2^- \bullet B \xrightarrow{fast} A_2^- + B$ $A_2 \bullet B_2 + NO_3^- \not\rightarrow A_2^- \bullet B_2$	All bases: $A_1^- + A_1 \xrightarrow{k_c} A_2^-$ $A_1^- + A_1 \bullet B \xrightarrow{k_c} A_2^- \bullet B$

Trimer, N_3 :

Neutral trimers (N_3) are primarily formed by combining one of the two types of monomers with one of the two types of dimers; evaporation of large clusters also contributes. In the sulfuric acid+DMA system, computational chemistry predicts $A_3 \bullet DMA_2$ and $A_3 \bullet DMA_3$ are relatively stable, with $A_3 \bullet DMA_3$ exhibiting the lowest evaporation rate (Ortega et al., 2012). Also $A_3 \bullet DMA$ may be present in significant amounts due to a high production rate via $A_2 \bullet DMA + A_1$. CI of N_3 leads to ions such as (i) $A_3^- \bullet DMA_3$ which evaporate at a rate of 10^4 s^{-1} into $A_3^- \bullet DMA_2$ and (ii) $A_3^- \bullet DMA_2$ and $A_3^- \bullet DMA$ which have predicted **DMA** evaporation rates of $\sim 10^{-1}$ and 10^{-2} s^{-1} (Ortega et al., 2014), respectively, resulting in lifetimes comparable to t_{CI} used here. From **Figure 1** ~~Figure 4~~, nitrate CI resulted in $A_3^- \bullet DMA_2$ (only at $[DMA]=110$ pptv), $A_3^- \bullet DMA$, and A_3^- . The DMA-containing clusters were detected to a much lesser extent than with acetate CI.

Acetate CI results help shed light on these processes with much higher $[A_3^- \bullet DMA_{1,2}]$ than with nitrate CI (Figure 1) which could be due to decomposition of larger ion clusters. The acetate CI results depicted in Figure 1 show that $A_3^- \bullet DMA_2$ is the most abundant type of trimer ion, suggesting that the dominant neutral clusters are $A_3 \bullet DMA_{2,3}$, with any $A_3 \bullet DMA_3$ quickly decomposing into $A_3 \bullet DMA_2$. Neutral $A_3 \bullet DMA_3$ is predicted by our model to be dominant at high $[DMA]$. This picture is consistent with our postulate that nitrate cannot ionize $A_3 \bullet DMA_3$ (and also, possibly, $A_3 \bullet DMA_2$) and thus little $A_3^- \bullet DMA_{1,2}$ is observed using nitrate CI.

The trimer ions observed using acetate CI may have contributions from decomposition of large clusters. For example, $A_3^- \bullet DMA_2$ could be formed by the decomposition of $A_4^- \bullet DMA_2$ or $A_4^- \bullet DMA_3$ via loss of A_1 or $A_1 \bullet DMA$, respectively. If these types of processes are significant, they might explain some of the differences in the trimer ion observations between nitrate and acetate CI. Highly aminated tetramer neutrals would be more readily ionized by acetate and result in larger contributions to the trimer ion signals than compared nitrate CI. Thus, this may be one drawback to acetate CI: a possible shift downwards in sulfuric acid content in the distribution of ions vs. the neutrals.

The sulfuric acid + diamine system shows nitrate CI detection of $A_3^+ \cdot \text{diamine}_{0.2}$ but at much lower abundances than acetate CI, particularly for EDA. Interestingly, the most abundant trimer ions after acetate CI contain on average 1 diamine molecule compared to 2 in the DMA system. This is consistent with particle measurements that show one diamine molecule is able to stabilize several sulfuric acid molecules, and thus form a stable particle, while at least 2 DMA molecules are required for the same effect (Jen et al., 2016). The two amino groups on the diamine molecule can both effectively stabilize trimers, and this size is stable for the relevant time scales in this flow reactor (Glasoe et al., 2015; Jen et al., 2016). Therefore, larger clusters can be produced with higher acid to base ratios.

To better understand the trimer ion behaviors, we monitored the bare trimer signal (A_3^+ , S_{293}) and monomer signal (S_{160}) as a function of CI reaction time, t_{CI} . Figure 8 shows S_{293}/S_{160} for nitrate CI for DMA, EDA, and TMEDA at $[A_1]_0 = 4 \times 10^9 \text{ cm}^{-3}$. Note, equivalent measurements for Put are similar to those of EDA. Low values of S_{293}/S_{160} for all conditions indicate minimal creation of A_3^+ from the CI of N_3 . Thus, IIC-produced A_3^+ can be a significant fraction of observed A_3^+ . Without base present, IIC is the only way to produce detectable amounts of A_3^+ (green circles in Figure 8).

A_3^+ can also be formed by the decomposition of larger ions such as $A_3^+ \cdot B$. Evidence of this decomposition can be seen in Figure 9 where S_{A_3+B}/S_{160} measured using nitrate CI is shown as a function of t_{CI} . For diamines at high concentrations and short t_{CI} , S_{A_3+B}/S_{160} decreases with t_{CI} and can be attributed to decomposition of this ion. Shorter t_{CI} allows the instrument to capture short-lived ions. $A_3^+ \cdot \text{diamine}$ decomposes at longer times and could form A_3^+ , thereby decreasing S_{A_3+B}/S_{160} and increasing S_{293}/S_{160} . However, S_{293}/S_{160} for the diamines does not increase with t_{CI} , indicating that $A_3^+ \cdot \text{diamine}$ likely decomposes into products other than A_3^+ . The DMA system also exhibits a very small decrease of S_{A_3+B}/S_{160} at short t_{CI} , but ratio values are within measurement uncertainties. Thus no conclusion can be drawn from this decrease of S_{A_3+B}/S_{160} at short t_{CI} .

Another, more likely scenario to explain these time dependent behaviors for the trimer ion signals is if $A_3^+ \cdot B$ decays into A_2^+ and a neutral $A_1 \cdot B$ at short t_{CI} . Assuming we have captured most of the initial $A_3^+ \cdot B$ signal at the shortest $t_{CI} = 15 \text{ ms}$ in Figure 9 (a-c), the increase in A_2^+ due to this mechanism would be small compared to the observed A_2^+ signal. Acetate data for Put (Figure 7 c) provide some evidence supporting this because the slope of the [Put]=2 pptv is 3.7 and is higher than the 2.6 slope of [B]=0 pptv case. Since A_2^+ when [B]=0 pptv is primarily produced by IIC, a higher slope when [Put]=2 pptv indicates larger ion decomposition contributing to the A_2^+ signal.

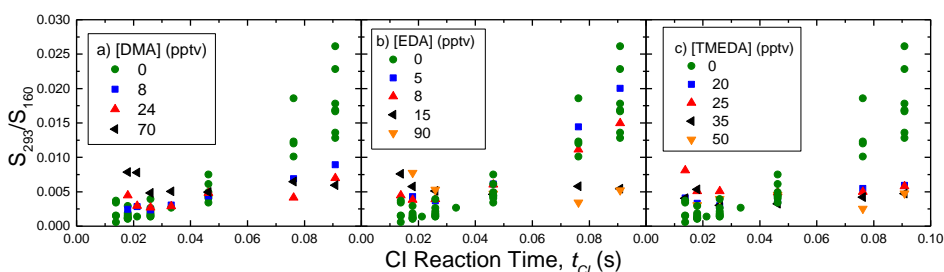


Figure 8 Measured bare sulfuric acid trimer to monomer signal ratio (S_{293}/S_{160}) as a function of t_{CI} for DMA (a), EDA (b), and TMEDA (c) detected by nitrate CI at $[A_1]_0 = 4 \times 10^9 \text{ cm}^{-3}$.

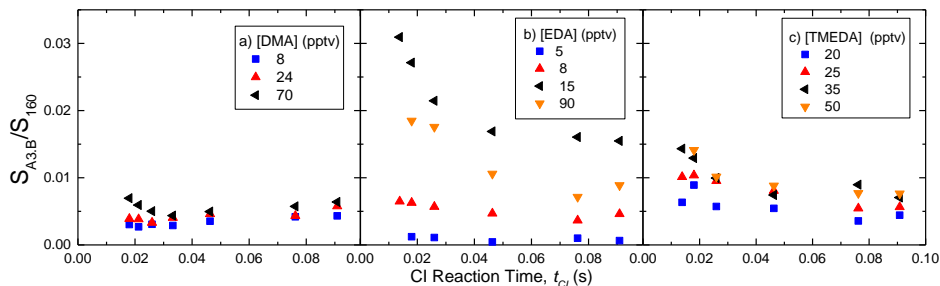


Figure 9 Nitrate measured signal ratio between $A_3 \bullet B$ and sulfuric acid monomer (S_{A_3B}/S_{160}) as a function of t_{CI} for DMA (a), EDA (b), and TMEDA (c) at $[A_1]_0 = 4 \times 10^9 \text{ cm}^{-3}$. *Note the different y-axis scales between bases.*

Scenarios deduced from these trimer ion observations and previous computational chemistry studies for the sulfuric acid and DMA system are summarized in Table 3. These reactions have little effect on the modeled dimer results since they introduce minor sources of dimer ions sources. In contrast, each trimer pathway adds large uncertainty to the modeled trimer behavior. For example, including ion decomposition reactions of larger ions (tetramer and larger), postulated from the acetate CI results, may greatly influence concentration of smaller trimer ions which already exhibit very low signals using nitrate CI. In addition, nitrate inefficient ionization of neutral trimers leads to large uncertainties in modeling the unobserved trimer types. More detailed observations of the chemically neutral trimers and computational chemistry studies on evaporation rates for sulfuric acid+diamine systems will improve future efforts to model these processes.

Table 3 Summary of possible pathways for neutral and ion trimers formed from sulfuric acid and DMA, excluding decomposition of tetramer and larger ions

Neutral formation	Nitrate CI and ion decomposition reactions	IIC reactions (only A_1^-)
$A_2 \bullet B + A_1 \xrightarrow{k} A_3 \bullet B$	$A_3 \bullet B + NO_3^- \xrightarrow{k_c} A_3^- \bullet B + HNO_3$	$A_2^- + A_1 \xrightarrow{k_c} A_3^-$
$A_3 \bullet B + B \xrightarrow{k} A_3 \bullet B_2$	$A_3^- \bullet B \xrightarrow{E_d} A_2^- + A_1 \bullet B$	$A_1^- + A_2 \bullet B \xrightarrow{k_c} A_3^- \bullet B$
$A_3 \bullet B_2 + B \xrightarrow{k} A_3 \bullet B_3$	$A_3 \bullet B_3 + NO_3^- \nrightarrow A_3^- \bullet B_3 + HNO_3$	
$A_2 \bullet B_2 + A_1 \xrightarrow{k} A_3 \bullet B_2$	$A_3 \bullet B_2 + NO_3^- \nrightarrow A_3^- \bullet B_2 + HNO_3$	
$A_2 \bullet B + A_1 \bullet B \xrightarrow{k} A_3 \bullet B_2$		
$A_2 \bullet B_2 + A_1 \bullet B \xrightarrow{k} A_3 \bullet B_3$		

Tetramer, N_4 :

Nitrate CI leads to very low amounts of tetramer ions and primarily as $A_4 \bullet \text{DMA}_{1-3}$ and $A_4 \bullet \text{diamine}_{1,2}$. Computational chemistry suggests that the sulfuric acid+DMA tetramer likely exists as $A_4 \bullet \text{DMA}_{2-4}$, with $A_4 \bullet \text{DMA}_4$ dominating the population (Ortega et al., 2012). The acetate data appears to confirm this with $A_4 \bullet \text{DMA}_3$ as the most abundant tetramer ion which likely predominately originated from the decomposition of $A_4 \bullet \text{DMA}_4$ upon ionization (Ortega et al., 2014). Nitrate may efficiently chemically ionize $A_4 \bullet \text{DMA}_{1-2}$, however their concentrations after the 3 s neutral reaction time are likely below the detection limit of the Cluster CIMS ($< 10^5 \text{ cm}^{-3}$). Furthermore, the $A_4^- \bullet \text{DMA}_{1,2}$ ions may be subject to elimination of $A_1 \bullet \text{DMA}$. Nitrate CI results show ~ 100 times higher $[A_4 \bullet \text{diamine}]$

Formatted: Subscript

than $[A_4 \cdot \text{DMA}]$ at about equivalent initial reactant concentrations. This suggests that the most stable neutral tetramers contain fewer diamine molecules than DMA. In addition, the acetate CI results for the diamines show the majority of N_4 contain 1 diamine, further supporting the conclusions drawn in Jen et al. (2016) that only one diamine molecule is needed to form a stable particle.

Due to the very low observed concentration of $A_4 \cdot \text{DMA}$, we focus on the ions of the diamine systems. The stability and behavior of $A_4 \cdot \text{diamine}$ can be examined by looking at nitrate detected signal ratios of $A_4 \cdot \text{diamine}$ and the monomer ($S_{A_4 \cdot \text{diamine}}/S_{160}$) as a function of CI reaction time, given in Figure 10. Similar to $A_3 \cdot \text{EDA}$, $S_{A_4 \cdot \text{EDA}}/S_{160}$ and $S_{A_4 \cdot \text{Put}}/S_{160}$ decreases with time at short t_{CI} , indicating that they decompose with a lifetime shorter than a few tens of ms. $S_{A_4 \cdot \text{TMEDA}}/S_{160}$ also shows a decrease at short t_{CI} , but it is less evident. It could have a fast decay rate leading to a few ms lifetime, and our measurements would have mostly missed them. Nonetheless, decomposition of $A_4 \cdot \text{diamine}$ likely entails evaporation of N_1 or N_2 instead of a lone diamine from the cluster as $[A_4]$ was below detection limit of the Cluster CIMS using nitrate. At long CI reaction time, $S_{A_4 \cdot \text{EDA}}/S_{160}$ remained constant, indicating negligible contribution of IIC to $A_4 \cdot \text{EDA}$ signal. In contrast, $S_{A_4 \cdot \text{Put}}/S_{160}$ and $S_{A_4 \cdot \text{TMEDA}}/S_{160}$ increase at long t_{CI} . This could be due to IIC or larger ion decomposition.

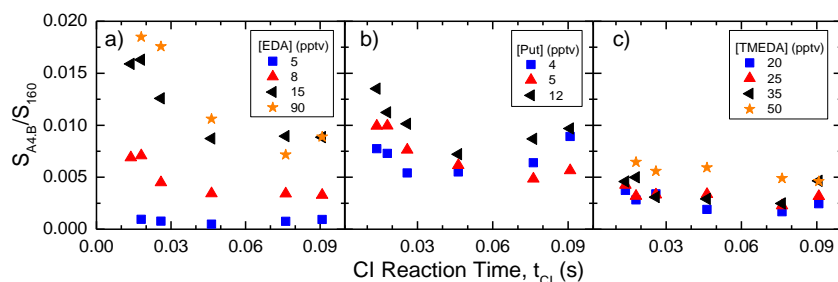


Figure 10 Nitrate measured signal ratio between $A_4 \cdot B$ and sulfuric acid monomer ($S_{A_4 \cdot \text{diamine}}/S_{160}$) as a function of CI reaction time for EDA (a), Put (b), and TMEDA (c).

Formatted: Subscript

Pentamer, N_5 :

Nitrate CI did not detect any pentamer (N_5), but pentamer was detected using acetate CI. In the diamine system, acetate detected N_5 with fewer diamine molecules (1-2) than DMA (4). However, $A_5 \cdot \text{EDA}_{>3}$, $A_5 \cdot \text{TMEDA}_{>1}$, and $A_5 \cdot \text{Put}_{>2}$ fall outside the Cluster CIMS mass range of 710 amu. Thus, we may not have measured the complete pentamer population. The most abundant N_5 is $A_5 \cdot \text{DMA}_4$ and it increases in both concentration and in fraction of N_5 population with increasing [DMA]. This ion could be the result of the loss of a DMA molecule after CI of $A_5 \cdot \text{DMA}_5$. This would follow similar trends predicted by computation chemistry for smaller clusters. However, since $[\text{DMA}] \ll [A_1]_0$ (i.e., $[B]/[A_1]_0$ is high) and stable particles need ~ 2 DMA to form (Glasoe et al., 2015), $[A_5 \cdot \text{DMA}_5]$ as high as 10^7 cm^{-3} would not be expected. The presence of $A_5 \cdot \text{DMA}_4$ could also then be the result of large ion decomposition via evaporation of A_1 or $A_1 \cdot \text{DMA}$. Measurements of ions larger than 700 amu are needed to better understand how they evaporate upon acetate CI and what fraction of the pentamers are not ionizable by nitrate.

Conclusion:

This study presents measurements of the behavior of neutral and ionized sulfuric acid clusters containing various bases. The results show the complexities of the coupled neutral cluster formation pathways with the ion processes (e.g. chemical ionization, ion-induced clustering, and ion decomposition). We provide various scenarios to describe the observed trends. Our most definitive conclusions are

- 1) Nitrate very likely does not chemically ionize all types of sulfuric acid dimers containing diamines. The model indicates $A_2 \cdot \text{diamine}_2$ cannot be chemically ionized by nitrate. However, the model did not consider semi-efficient nitrate CI of $A_2 \cdot \text{diamine}$ which could also explain our observations.
- 2) Nitrate only chemically ionizes a small fraction of trimer and larger clusters in both the DMA and diamine with sulfuric acid systems. Measurements suggest that the more chemically neutral clusters are not chemically ionized by nitrate but are by acetate.
- 3) Acetate and nitrate CI measurements of sulfuric acid+DMA clusters generally agree with the qualitative trends of neutral and ion cluster predicted from computational chemistry (Ortega et al., 2012; Ortega et al., 2014). However, these measurements suggest that $A_3 \cdot B$ decomposes into A_2^- and $A_1 \cdot B$.
- 4) Nitrate measurements of $A_3 \cdot B$ and $A_4 \cdot B$ show that these ions decompose at roughly the same time scales as the CI reaction time at room temperature. In principle, ionization of neutral clusters leads to potentially large artifacts even before they are sampled into a vacuum system. These decomposition reactions will likely affect the calculated concentrations of the neutral clusters.
- 5) In an acid-rich environment where $[B]/[A_1] < 1$, A_2^- and A_3^- are primarily produced via IIC pathways and contribute negligible amounts to overall dimer and trimer signals when any of these bases are present and at our 18 ms CI reaction time. If some fraction of the dimer is not chemically ionized by nitrate, then IIC-produced A_2^- is a significant fraction of the dimer signal.

Additional computed neutral and ion evaporation rates and a more complex model combined with multivariable parameter fitting would provide more clarity to these results. In addition, more acetate CI measurements of ion signal ratios as a function of CI reaction time are needed to provide more details on specific ion behaviors. However, measurements using the acetate ion (which includes acetate, acetate•water, and acetic acid•acetate) exhibit high backgrounds in the low masses, leading to up to a factor of 5 uncertainty in measured monomer concentration ($[N_1]$) and a factor of 2-3 for dimer concentration ($[N_2]$). A higher resolution mass spectrometer is needed to resolve the background signals and reduce the uncertainties.

Acknowledgements:

Support from NSF Awards AGS1068201, AGS1338706, and AGS0943721 is gratefully acknowledged. CNJ acknowledges support from NSF GRFP award 00006595, UMN DDF, and NSF AGS Postdoctoral Fellowship award 1524211. J. Z. acknowledges support from SYSU 100 talents program.

References:

- Almeida, J., Schobesberger, S., Kurten, A., Ortega, I. K., Kupiainen-Maatta, O., Praplan, A. P., Adamov, A., Amorim, A., Bianchi, F., Breitenlechner, M., David, A., Dommen, J., Donahue, N. M., Downard, A., Dunne, E., Duplissy, J., Ehrhart, S., Flagan, R. C., Franchin, A., Guida, R., Hakala, J., Hansel, A., Heinritzi, M., Henschel, H., Jokinen, T., Junninen, H., Kajos, M., Kangasluoma, J., Keskinen, H., Kupc, A., Kurten, T., Kvashin, A. N., Laaksonen, A., Lehtipalo, K., Leiminger, M., Leppa, J., Loukonen, V., Makhmutov, V., Mathot, S., McGrath, M. J., Nieminen, T., Olenius, T., Onnela, A., Petaja, T., Riccobono, F., Riipinen, I., Rissanen, M., Rondo, L., Ruuskanen, T., Santos, F. D., Sarnela, N., Schallhart, S., Schnitzhofer, R., Seinfeld, J. H., Simon, M., Sipila, M., Stozhkov, Y., Stratmann, F., Tome, A., Trostl, J., Tsagkogeorgas, G., Vaattovaara, P., Viisanen, Y., Virtanen, A., Vrtala, A., Wagner, P. E., Weingartner, E., Wex, H., Williamson, C., Wimmer, D., Ye, P., Yli-Juuti, T., Carslaw, K. S., Kulmala, M., Curtius, J., Baltensperger, U., Worsnop, D. R., Vehkamäki, H., and Kirkby, J.: Molecular understanding of sulphuric acid-amine particle nucleation in the atmosphere, *Nature*, 502, 359-363, 10.1038/nature12663, 2013.
- Ball, S. M., Hanson, D. R., Eisele, F. L., and McMurry, P. H.: Laboratory studies of particle nucleation: Initial results for H_2SO_4 , H_2O , and NH_3 vapors, *Journal of Geophysical Research: Atmospheres*, 104, 23709-23718, 10.1029/1999JD900411, 1999.
- Berresheim, H., Elste, T., Plass-Dülmer, C., Eisele, F. L., and Tanner, D. J.: Chemical ionization mass spectrometer for long-term measurements of atmospheric OH and H_2SO_4 , *International Journal of Mass Spectrometry*, 202, 91-109, 10.1016/s1387-3806(00)00233-5, 2000.
- Bork, N., Elm, J., Olenius, T., and Vehkamäki, H.: Methane sulfonic acid-enhanced formation of molecular clusters of sulfuric acid and dimethyl amine, *Atmos. Chem. Phys.*, 14, 12023-12030, 10.5194/acp-14-12023-2014, 2014.
- Chen, M., Titcombe, M., Jiang, J., Jen, C., Kuang, C., Fischer, M. L., Eisele, F. L., Siepmann, J. I., Hanson, D. R., Zhao, J., and McMurry, P. H.: Acid-base chemical reaction model for nucleation rates in the polluted atmospheric boundary layer, *Proceedings of the National Academy of Sciences*, 109, 18713-18718, 10.1073/pnas.1210285109, 2012.
- Coffman, D. J., and Hegg, D. A.: A preliminary study of the effect of ammonia on particle nucleation in the marine boundary layer, *Journal of Geophysical Research: Atmospheres*, 100, 7147-7160, 10.1029/94JD03253, 1995.
- Eisele, F. L., and Hanson, D. R.: First Measurement of Prenucleation Molecular Clusters, *The Journal of Physical Chemistry A*, 104, 830-836, 10.1021/jp9930651, 2000.
- Elm, J., Jen, C. N., Kurtén, T., and Vehkamäki, H.: Strong Hydrogen Bonded Molecular Interactions between Atmospheric Diamines and Sulfuric Acid, *The Journal of Physical Chemistry A*, 120, 3693-3700, 10.1021/acs.jpca.6b03192, 2016.
- Freshour, N., Carlson, K., Melka, Y. A., Hinz, S., and Hanson, D. R.: Quantifying Amine Permeation Sources with Acid Neutralization: AmPMS Calibrations and Amines in Coastal and Continental Atmospheres, *Atmos. Meas. Tech.*, 7, 3611-3621, 10.5194/amt-7-3611-2014, 2014.
- Glasoe, W. A., Volz, K., Panta, B., Freshour, N., Bachman, R., Hanson, D. R., McMurry, P. H., and Jen, C.: Sulfuric Acid Nucleation: An Experimental Study of the Effect of Seven Bases, *Journal of Geophysical Research: Atmospheres*, 1933-1950, 10.1002/2014JD022730, 2015.
- Hanson, D. R., and Eisele, F. L.: Measurement of prenucleation molecular clusters in the NH_3 , H_2SO_4 , H_2O system, *J. Geophys. Res.*, 107, AAC 10-11 - AAC 10-18, 10.1029/2001jd001100, 2002.
- Hanson, D. R., and Lovejoy, E. R.: Measurement of the Thermodynamics of the Hydrated Dimer and Trimer of Sulfuric Acid, *The Journal of Physical Chemistry A*, 110, 9525-9528, 10.1021/jp062844w, 2006.
- IPCC: Climate Change 2014: Impacts, Adaptation, and Vulnerability. Part A: Global and Sectoral Aspects. Contribution of Working Group II to the Fifth Assessment Report of the Intergovernmental Panel on Climate Change [Field, C.B., V.R. Barros, D.J. Dokken, K.J. Mach, M.D. Mastrandrea, T.E. Bilir, M. Chatterjee, K.L. Ebi, Y.O. Estrada, R.C. Genova, B. Girma, E.S. Kissel, A.N. Levy, S. MacCracken, P.R. Mastrandrea, and L.L. White (eds.)], Cambridge University Press, Cambridge, United Kingdom and New York, NY, USA, 1132 pp., 2014.
- Jen, C. N., McMurry, P. H., and Hanson, D. R.: Stabilization of sulfuric acid dimers by ammonia, methylamine, dimethylamine, and trimethylamine, *Journal of Geophysical Research: Atmospheres*, 119, 7502-7514, 10.1002/2014JD021592, 2014.
- Jen, C. N., Hanson, D. R., and McMurry, P. H.: Towards Reconciling Measurements of Atmospherically Relevant Clusters by Chemical Ionization Mass Spectrometry and Mobility Classification/Vapor Condensation, *Aerosol Science and Technology*, ARL, 49, i-iii, 10.1080/02786826.2014.1002602, 2015.

578 Jen, C. N., Bachman, R., Zhao, J., McMurry, P. H., and Hanson, D. R.: Diamine-sulfuric acid reactions are a potent
579 source of new particle formation, *Geophysical Research Letters*, 43, 867–873, 10.1002/2015GL066958, 2016.

580 Jiang, J., Zhao, J., Chen, M., Eisele, F. L., Scheckman, J., Williams, B. J., Kuang, C., and McMurry, P. H.: First
581 Measurements of Neutral Atmospheric Cluster and 1–2 nm Particle Number Size Distributions During Nucleation
582 Events, *Aerosol Science and Technology*, 45, ii–v, 10.1080/02786826.2010.546817, 2011.

583 Jokinen, T., Sipilä, M., Junninen, H., Ehn, M., Lönn, G., Hakala, J., Petäjä, T., Mauldin Iii, R. L., Kulmala, M., and
584 Worsnop, D. R.: Atmospheric sulphuric acid and neutral cluster measurements using CI-API-TOF, *Atmos. Chem.*
585 *Phys.*, 12, 4117–4125, 10.5194/acp-12-4117-2012, 2012.

586 Kirkby, J., Curtius, J., Almeida, J., Dunne, E., Duplissy, J., Franchin, A., Gagne, S., Ickes, L., Kurten, A.,
587 Kupc, A., Metzger, A., Riccobono, F., Rondo, L., Schobesberger, S., Tsagkogeorgas, G., Wimmer, D., Amorim,
588 A., Bianchi, F., Breitenlechner, M., David, A., Dommen, J., Downard, A., Ehn, M., Flagan, R. C., Haider, S.,
589 Hansel, A., Hauser, D., Jud, W., Junninen, H., Kreissl, F., Kvashin, A., Laaksonen, A., Lehtipalo, K., Lima, J.,
590 Lovejoy, E. R., Makhmutov, V., Mathot, S., Mikkilä, J., Minginette, P., Mogo, S., Nieminen, T., Onnela, A.,
591 Pereira, P., Petaja, T., Schnitzhofer, R., Seinfeld, J. H., Sipilä, M., Stozhkov, Y., Stratmann, F., Tome, A.,
592 Vanhanen, J., Viisanen, Y., Vrtala, A., Wagner, P. E., Walther, H., Weingartner, E., Wex, H., Winkler, P. M.,
593 Carslaw, K. S., Worsnop, D. R., Baltensperger, U., and Kulmala, M.: Role of sulphuric acid, ammonia and
594 galactic cosmic rays in atmospheric aerosol nucleation, *Nature*, 476, 429–433, 10.1038/nature10343, 2011.

595 Kuang, C., McMurry, P. H., McCormick, A. V., and Eisele, F. L.: Dependence of nucleation rates on sulfuric acid
596 vapor concentration in diverse atmospheric locations, *Journal of Geophysical Research: Atmospheres*, 113,
597 10.1029/2007jd009253, 2008.

598 Kulmala, M., Vehkamäki, H., Petäjä, T., Dal Maso, M., Lauri, A., Kerminen, V. M., Birmili, W., and McMurry, P.
599 H.: Formation and growth rates of ultrafine atmospheric particles: a review of observations, *Journal of Aerosol*
600 *Science*, 35, 143–176, 10.1016/j.jaerosci.2003.10.003, 2004.

601 Kürten, A., Jokinen, T., Simon, M., Sipilä, M., Sarnela, N., Junninen, H., Adamov, A., Almeida, J., Amorim, A.,
602 Bianchi, F., Breitenlechner, M., Dommen, J., Donahue, N. M., Duplissy, J., Ehrhart, S., Flagan, R. C., Franchin,
603 A., Hakala, J., Hansel, A., Heinritzi, M., Hutterli, M., Kangasluoma, J., Kirkby, J., Laaksonen, A., Lehtipalo, K.,
604 Leiminger, M., Makhmutov, V., Mathot, S., Onnela, A., Petäjä, T., Praplan, A. P., Riccobono, F., Rissanen, M.
605 P., Rondo, L., Schobesberger, S., Seinfeld, J. H., Steiner, G., Tomé, A., Tröstl, J., Winkler, P. M., Williamson,
606 C., Wimmer, D., Ye, P., Baltensperger, U., Carslaw, K. S., Kulmala, M., Worsnop, D. R., and Curtius, J.: Neutral
607 molecular cluster formation of sulfuric acid–dimethylamine observed in real time under atmospheric conditions,
608 *Proceedings of the National Academy of Sciences*, 111, 15019–15024 10.1073/pnas.1404853111, 2014.

609 Kurtén, T., Petäjä, T., Smith, J., Ortega, I. K., Sipilä, M., Junninen, H., Ehn, M., Vehkamäki, H., Mauldin, L.,
610 Worsnop, D. R., and Kulmala, M.: The effect of H₂SO₄ & amine clustering on chemical ionization mass
611 spectrometry (CIMS) measurements of gas-phase sulfuric acid, *Atmos. Chem. Phys.*, 11, 3007–3019,
612 10.5194/acp-11-3007-2011, 2011.

613 Leopold, K. R.: Hydrated Acid Clusters, *Annual Review of Physical Chemistry*, 62, 327–349, doi:10.1146/annurev-
614 physchem-032210-103409, 2011.

615 Leverentz, H. R., Siepmann, J. I., Truhlar, D. G., Loukonen, V., and Vehkamäki, H.: Energetics of Atmospherically
616 Implicated Clusters Made of Sulfuric Acid, Ammonia, and Dimethyl Amine, *The Journal of Physical Chemistry*
617 *A*, 117, 3819–3825, 10.1021/jp402346u, 2013.

618 Lovejoy, E. R., and Bianco, R.: Temperature Dependence of Cluster Ion Decomposition in a Quadrupole Ion Trap†,
619 *The Journal of Physical Chemistry A*, 104, 10280–10287, 10.1021/jp001216q, 2000.

620 Lovejoy, E. R., and Curtius, J.: Cluster Ion Thermal Decomposition (II): Master Equation Modeling in the Low-
621 Pressure Limit and Fall-Off Regions. Bond Energies for HSO₄-(H₂SO₄),(HNO₃)_n, *The Journal of Physical*
622 *Chemistry A*, 105, 10874–10883, 10.1021/jp012496s, 2001.

623 McGrath, M. J., Olenius, T., Ortega, I. K., Loukonen, V., Paasonen, P., Kurtén, T., Kulmala, M., and Vehkamäki, H.:
624 Atmospheric Cluster Dynamics Code: a flexible method for solution of the birth-death equations, *Atmos. Chem.*
625 *Phys.*, 12, 2345–2355, 10.5194/acp-12-2345-2012, 2012.

626 Nadykto, A. B., Herb, J., Yu, F., and Xu, Y.: Enhancement in the production of nucleating clusters due to
627 dimethylamine and large uncertainties in the thermochemistry of amine-enhanced nucleation, *Chemical Physics*
628 *Letters*, 609, 42–49, 10.1016/j.cplett.2014.03.036, 2014.

629 Ortega, I. K., Kupiainen, O., Kurtén, T., Olenius, T., Wilkman, O., McGrath, M. J., Loukonen, V., and Vehkamäki,
630 H.: From quantum chemical formation free energies to evaporation rates, *Atmos. Chem. Phys.*, 12, 225–235,
631 10.5194/acp-12-225-2012, 2012.

- Ortega, I. K., Olenius, T., Kupiainen-Määttä, O., Loukonen, V., Kurtén, T., and Vehkamäki, H.: Electrical charging changes the composition of sulfuric acid–ammonia/dimethylamine clusters, *Atmos. Chem. Phys.*, 14, 7995–8007, 10.5194/acp-14-7995-2014, 2014.
- Riipinen, I., Sihto, S. L., Kulmala, M., Arnold, F., Dal Maso, M., Birmili, W., Saarnio, K., Teinilä, K., Kerminen, V. M., Laaksonen, A., and Lehtinen, K. E. J.: Connections between atmospheric sulphuric acid and new particle formation during QUEST III-IV campaigns in Heidelberg and Hyytiälä, *Atmos. Chem. Phys.*, 7, 1899–1914, 10.5194/acp-7-1899-2007, 2007.
- Schobesberger, S., Junninen, H., Bianchi, F., Lönn, G., Ehn, M., Lehtipalo, K., Dommen, J., Ehrhart, S., Ortega, I. K., Franchin, A., Nieminen, T., Riccobono, F., Hutterli, M., Duplissy, J., Almeida, J., Amorim, A., Breitenlechner, M., Downard, A. J., Dunne, E. M., Flagan, R. C., Kajos, M., Keskinen, H., Kirkby, J., Kupc, A., Kürten, A., Kurtén, T., Laaksonen, A., Mathot, S., Onnela, A., Praplan, A. P., Rondo, L., Santos, F. D., Schallhart, S., Schnitzhofer, R., Sipilä, M., Tomé, A., Tsagkogeorgas, G., Vehkamäki, H., Wimmer, D., Baltensperger, U., Carslaw, K. S., Curtius, J., Hansel, A., Petäjä, T., Kulmala, M., Donahue, N. M., and Worsnop, D. R.: Molecular understanding of atmospheric particle formation from sulfuric acid and large oxidized organic molecules, *Proceedings of the National Academy of Sciences*, 110, 17223–17228, 10.1073/pnas.1306973110, 2013.
- Su, T., and Bowers, M. T.: Theory of ion-polar molecule collisions. Comparison with experimental charge transfer reactions of rare gas ions to geometric isomers of difluorobenzene and dichloroethylene, *The Journal of Chemical Physics*, 58, 3027–3037, 10.1063/1.1679615, 1973.
- Veres, P., Roberts, J. M., Warneke, C., Welsh-Bon, D., Zahniser, M., Herndon, S., Fall, R., and de Gouw, J.: Development of negative-ion proton-transfer chemical-ionization mass spectrometry (NI-PT-CIMS) for the measurement of gas-phase organic acids in the atmosphere, *International Journal of Mass Spectrometry*, 274, 48–55, 10.1016/j.ijms.2008.04.032, 2008.
- Viggiano, A. A., Seeley, J. V., Mundis, P. L., Williamson, J. S., and Morris, R. A.: Rate Constants for the Reactions of $\text{XO}_3^-(\text{H}_2\text{O})_n$ ($\text{X} = \text{C}, \text{HC}, \text{and N}$) and $\text{NO}_3^-(\text{HNO}_3)_n$ with H_2SO_4 : Implications for Atmospheric Detection of H_2SO_4 , *The Journal of Physical Chemistry A*, 101, 8275–8278, 10.1021/jp971768h, 1997.
- Weber, R. J., Marti, J. J., McMurry, P. H., Eisele, F. L., Tanner, D. J., and Jefferson, A.: Measured atmospheric new particle formation rates: implications for nucleation mechanisms, *Chemical Engineering Communications*, 151, 53–64, 10.1080/00986449608936541, 1996.
- Zhao, J., Eisele, F. L., Titcombe, M., Kuang, C., and McMurry, P. H.: Chemical ionization mass spectrometric measurements of atmospheric neutral clusters using the cluster-CIMS, *J. Geophys. Res.*, 115, 10.1029/2009jd012606, 2010.
- Zhao, J., Smith, J. N., Eisele, F. L., Chen, M., Kuang, C., and McMurry, P. H.: Observation of neutral sulfuric acid–amine containing clusters in laboratory and ambient measurements, *Atmos. Chem. Phys.*, 11, 10823–10836, 10.5194/acp-11-10823-2011, 2011.
- Zollner, J. H., Glasoe, W. A., Panta, B., Carlson, K. K., McMurry, P. H., and Hanson, D. R.: Sulfuric acid nucleation: power dependencies, variation with relative humidity, and effect of bases, *Atmos. Chem. Phys.*, 12, 4399–4411, 10.5194/acp-12-4399-2012, 2012.

Chemical ionization of clusters formed from sulfuric acid and dimethylamine or diamines

Coty N. Jen^{1,2*}, Jun Zhao^{1,3}, Peter H. McMurry¹, David R. Hanson⁴

¹Department of Mechanical Engineering, University of Minnesota – Twin Cities, 111 Church St. SE, Minneapolis, MN, 55455, USA

² now at Department of Environmental Science, Policy, and Management, University of California, Berkeley, Hilgard Hall, Berkeley, CA, 94720

³ now at Institute of Earth Climate and Environment System, Sun Yat-sen University, 135 West Xingang Road, Guangzhou 510275, China

⁴Department of Chemistry, Augsburg College, 2211 Riverside Ave., Minneapolis, MN, 55454, USA

*corresponding author email: jenco@berkeley.edu

Supporting Information:

- S1. Mass-dependent sensitivity of the Cluster CIMS
- S2. Nitrate vs. acetate mass spectra comparison for sulfuric acid+diamine
- S3. [N₁] and [N₂] from mass spectrometer signals
- S4. Modeled reactions and parameters

S1. Mass-dependent sensitivity of the Cluster CIMS:

Mass-dependent sensitivity experiments were performed on the University of MN Cluster CIMS following a near identical procedure as detailed in Zhao et al. (2010), with pertinent details described here. Four tetra-alkyl ammonium halide salts were used in this experiment: tetramethyl ammonium iodide (TMAI at 74 and 275 amu), tetrapropyl ammonium iodide (TPAI at 186 amu), tetrabutyl ammonium iodide (TBAI at 242 amu), and tetraheptyl ammonium bromide (THAB at 410 amu). These salts were dissolved in methanol and electrosprayed in positive ion mode. Specific ion mobilities (Ude and de la Mora, 2005) were selected using a high resolution differential mobility analyzer (HDMA) (Rosser and de la Mora, 2005). The flow containing mono-mobile ions was split into two equal streams with one measured by an electrometer and the other by the Cluster CIMS. The ions were directly delivered to the inlet of the Cluster CIMS where they first entered a conical octopole (1 MHz and 24 V pk-pk) then the quadrupole mass analyzer. The signals of the Cluster CIMS were then divided by the electrometer measured concentrations to obtain the sensitivity. Since the ions were delivered directly to the Cluster CIMS inlet, these experiments only probe the mass-dependent sensitivity of the inlet, octopole, quadrupole, and detector.

Figure S1 shows measured sensitivity at specific masses corresponding to the alkyl halide positive ions (black squares). We assume the mass-dependent sensitivity for positive ions is the same for negative ions. The sensitivity at smaller masses is lower than at larger masses, indicating that the Cluster CIMS more efficiently measures larger ions. For masses between 410 to 710 amu, we assume a sensitivity value of 0.037 Hz cm⁻³ (green line). Masses larger than 710 amu are not detected (i.e., sensitivity of zero) due to limits of our quadrupole. A constant sensitivity assumes that all mass from ~200-710 amu are measured with equal

Formatted: Font: 12 pt

Formatted: Superscript

efficiency. This contrasts with Zhao et al. (2010) where they observed a steep decline in sensitivity at large masses. We based our assumption on the size and shape of largest mass peaks. **Figure S2** shows a sample mass scan of sulfuric acid with $[EDA]=60$ pptv. The largest ion detected is $A_6 \cdot EDA_2$ at 707 amu. The peak is ~ 4 amu wide and ~ 600 Hz tall. If the sensitivity for this large ion were low, then the resulting $[A_6 \cdot EDA_2]$ would exceed that of $[A_2^-]$, an unlikely scenario.

The uncertainties associated with the sensitivity depend on the ion masses being compared. For ions similar in mass, such as $HNO_3 \cdot NO_3^-$ (125 amu) and $HNO_3 \cdot HSO_4^-$ (160 amu), the uncertainty is small at $\sim 20\%$. However, taking the ratio between various sulfuric acid clusters and the acetate reagent ion signals can result in uncertainties up to a factor of 2 to 3. This large uncertainty is due to extrapolating between the two smallest ion masses studied in the sensitivity measurements: 74 to 186 amu. In addition, the acetate reagent ions are all very small and fall on the steep rise of the sensitivity curve. More sensitivity experiments are required in the low mass range to reduce this uncertainty.

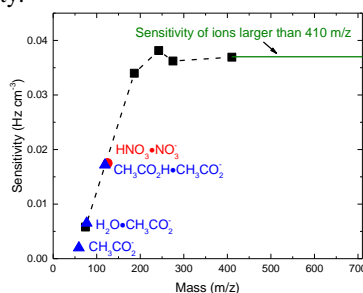


Figure S1 Sensitivity of the UMN Cluster CIMS as a function of mass. The black squares indicate the measured sensitivity of the positive alkyl halide ions. The blue triangles show the predicted sensitive of the acetate ions with three different ligands. The red circle is the sensitivity of the nitrate dimer ion. The dark green line is the extrapolated sensitivity for masses larger than 410 amu.

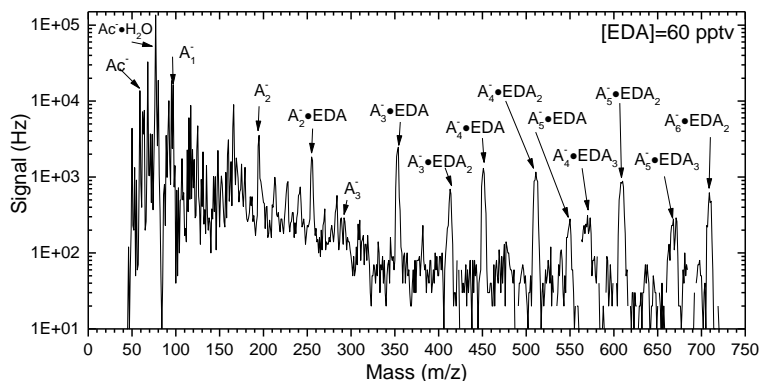


Figure S2 Mass scan of sulfuric acid at $[A_1]_0=4 \times 10^9 \text{ cm}^{-3}$ and $[EDA]=60$ pptv measured using acetate (Ac^-). Identities of sulfuric acid+EDA peaks are labeled.

Formatted: Font: 12 pt

S2. Nitrate vs. acetate mass spectra comparison for sulfuric acid+diamine

Figure S3 compares nitrate and acetate mass spectra for the three diamines at equivalent $[A_1]_0$ and $[B]$. As no other parameters of the Cluster CIMS changed between nitrate and acetate measurements, Figure S3 clearly shows that nitrate does not chemically ionize all types of sulfuric clusters in the presence of diamines. It is possible that larger ion clusters decompose to a greater extent with acetate CI than nitrate and lead to increased signal for the clusters shown in Figure S3. However, normalized acetate signals are 10 times larger than nitrate signals which would require very high and nonsensical concentrations of the larger clusters for decomposition to be the sole reason for the difference. Furthermore, nitrate detects small amounts of A_3^- •diamine; this could be due to decomposition of larger ions, IIC from $N_2+A_1^-$, or partially efficient nitrate CI of A_3^- •diamine.

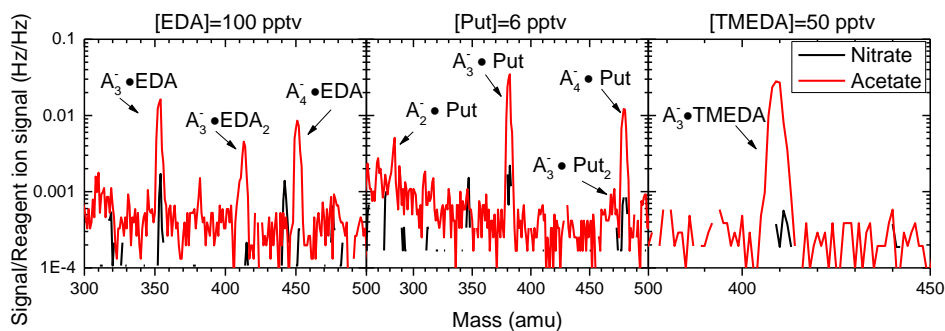


Figure S3 Comparison between nitrate (black) and acetate (red) mass spectra for EDA (left), Put (center), and TMEDA (right). The concentration of diamine for the comparison is given at the top of each panel.

S3. $[N_1]$ and $[N_2]$ from mass spectrometer signals

The depletion of the reagent ion (given here as $[NO_3^-]$) can be written as

$$\frac{d[NO_3^-]}{dt_{CI}} = -k_1[N_1][NO_3^-] \quad \text{Equation S1}$$

This assumes that the reagent ion only reacts with N_1 . This has a solution of

$$[NO_3^-] = [NO_3^-]_0 \exp(-k_1[N_1]t_{CI}) \quad \text{Equation S2}$$

Assuming $[A_1^-]$ is not formed in appreciable quantities by ion fragmentation, then the formation of $[A_1^-]$ can be written as

$$\frac{d[A_1^-]}{dt_{CI}} = k_1[N_1][NO_3^-] - k_{21}[A_1^-][N_1] \quad \text{Equation S3}$$

Substituting Equation S2 into Equation S3 gives

$$\frac{d[A_1^-]}{dt_{Cl}} = k_1[N_1][NO_3^-]_o \exp(-k_1[N_1]t_{Cl}) - k_{21}[A_1^-][N_1] \quad \text{Equation S4}$$

Where $[NO_3^-]_o$ is the initial concentration of NO_3^- . Equation S4 can be solved to give

$$[A_1^-] = k_1[NO_3^-]_o \left(\frac{\exp(-k_1[N_1]t_{Cl}) - \exp(-k_{21}[N_1]t_{Cl})}{k_{21} - k_1} \right) \quad \text{Equation S5}$$

Equation S2 can be inserted in Equation S5 to remove $[NO_3^-]_o$.

$$\frac{[A_1^-]}{[NO_3^-]} = \frac{S_{160}}{S_{125}} = \frac{k_1}{k_{21} - k_1} (1 - \exp((k_1 - k_{21})[N_1]t_{Cl})) \quad \text{Equation S6}$$

The signal at the ion's mass directly relates to the ion concentration (plus a mass-dependent sensitivity that we do not include in this derivation for simplicity but is included in the model); therefore, the $[A_1^-]$ can be replaced by S_{160} (bisulfate with a nitric acid ligand with a total mass of 160 amu) and $[NO_3^-]$ with S_{125} (nitrate with a nitric acid ligand for a mass of 125 amu).

Equation S6 is a more accurate method to convert signal ratios to neutral concentration then the equations given in Berresheim et al. (2000) and Eisele and Hanson (2000) as this equation does not assume constant concentrations of the reagent ion. However, at very short t_{Cl} (like the 15 to 18 ms used here), Equation S6 results in $[N_1]$ about 5% higher than using the logarithmic equation given in Berresheim et al. (2000) and 1% higher than the simple ratio equation of Eisele and Hanson (2000).

The derivation for $[A_2^-]$ (S_{195}) follows similar math as for $[A_1^-]$. The relation for $[A_2^-]$ as a function of t_{Cl} is given in Equation S7 and can be divided by Equation S5 to obtain S_{195}/S_{160} vs. t_{Cl} (not shown).

$$[A_2^-] = \frac{k_{21}k_1}{k_{21} - k_1} [NO_3^-]_o \left\{ \begin{aligned} &\exp(-k_1[N_1]t_{Cl}) / (k_{32} - k_1) + \exp(-k_{21}[N_1]t_{Cl}) / (k_{21} - k_{32}) \\ &- \exp(-k_{32}[N_1]t_{Cl}) / ((k_{32} - k_1)(k_{21} - k_{32})) \end{aligned} \right\} \quad \text{Equation S7}$$

Ratio of cluster signals to the reagent ion can be affected by several factors not considered in Equation S6. 1) Varying relative humidity alters the number of water ligands attached to charged and neutral clusters. This will alter the kinetics and stability of clusters, thus changing the amount and types of clusters detected. 2) The addition of base into the flow reactor introduces a small stream of nitrogen that may locally dilute $[N_1]$ by up to 40% with very high base addition flow rates prior to Cluster CIMS measurement. 3) Very high concentration of nitrate ion will allow more mixed clusters to be detected, i.e. $A_m^- \cdot B_j \cdot HNO_3$. Our measurements indicate that the stability of these clusters also depends on RH. 4) Prior to entering into the

vacuum region of the Cluster CIMS, the ions pass through a curtain gas flow consisting of 200 sccm of nitrogen. This flow slightly exceeds the flow into the mass spectrometer and may might cause ion clusters to evaporate. More information on cluster chemistry can be gained by studying how these factors alter observed clusters and their concentrations.

S4. Modeled reactions and parameters

The modeled reactions can be divided into three categories: neutral cluster formation, chemical ionization and ion decomposition, and IIC. ~~Table S2~~Table S2 lists all the reactions that were modeled. The neutral cluster forward rate constants, k , were assumed to be $4 \times 10^{-10} \text{ cm}^3 \text{ s}^{-1}$, and the ion forward rate constants, k_c , were taken to be $2 \times 10^{-9} \text{ cm}^3 \text{ s}^{-1}$. Some error is introduced in these forward rate constants but is likely small compared to other sources of uncertainty such as evaporation or decomposition rates. To constrain the number of parameters, we assumed ions either instantly decompose or do not decompose at all. Decomposition rate constants listed as *fast* were assumed to be instantaneous and the intermediate products do not form in appreciable quantities. Ion decomposition rate constants listed as E_{A,B_j} were assumed to be zero.

~~Table S1~~Table S1 provides the neutral cluster evaporation rates used for the model that produced good agreement with our observations. We examined numerous sets of neutral and ion evaporation rate combinations to determine if our measured signal ratios as a function of CI reaction time for the diamines could be explained by simple changes in evaporation rates. However, no sensible combination reproduced our observations, leading us to believe that some fraction of $[\text{N}_2]$ with diamines is not chemically ionized by nitrate.

These evaporation rates are by no means the “correct” rates. Our model only considered clusters up to size 4. The dynamics of the larger clusters likely effect the apparent evaporate rates of the smaller clusters. The evaporation rates also indicate that the clusters have lifetimes on the order of neutral reaction time of 3 s. Therefore, we cannot say with confidence that one of these four bases will stabilize clusters more than the others: they behave similarly during the 3 s reaction time. In addition, the evaporation rates are interconnected in the complex series of cluster balance equations. Different types of experiments, ones more sensitive to small differences in slow evaporation rates, are required to better quantify evaporation, decomposition, and partial chemical ionization rates.

Table S1 List of evaporation rates used for the model

Base	$E_1 \text{ (s}^{-1}\text{)}$	$E_{2B} \text{ (s}^{-1}\text{)}$	$E_2 \text{ (s}^{-1}\text{)}$	$E_{3A3B} \text{ (s}^{-1}\text{)}$	$E_{3A3B2} \text{ (s}^{-1}\text{)}$
DMA	0.1	0	0	1	1
EDA	5	0	0	0	0
Put	5	0	0	0	0
TMEDA	5	0	0	0	0

Formatted: Font: 12 pt

Formatted: Font: (Default) Times New Roman, 12 pt

Table S2 Summary of all the reactions modeled in this study. Note, reactions are unbalanced and written in shorthand.

Neutral cluster formation	CI and ion decomposition reactions	IIC reactions
$A_1 + B \xrightleftharpoons[E_1]{k} AB$ $AB + A_1 \xrightarrow{k} A_2B$ $AB + AB \xrightarrow{k} A_2B_2$ $A_2B + B \xrightarrow{k} A_2B_2$ $A_2B + A_1 \xrightarrow{k} A_3B$ $A_3B + B \xrightarrow{k} A_3B_2$ $A_3B_2 + B \xrightarrow{k} A_3B_3$ $A_2B_2 + A_1 \xrightarrow{k} A_3B_2$ $A_2B + AB \xrightarrow{k} A_3B_2$ $A_2B_2 + AB \xrightarrow{k} A_3B_3$ $A_3B_2 \xrightarrow{E_{A_3B_2}} A_2B_2 + A_1$ $A_3B \text{ or } A_3B_2 \text{ or } A_3B_3 + AB \xrightarrow{k} N_4$ $A_3B_2 \text{ or } A_3B_3 + A_1 \xrightarrow{k} N_4$ $A_2B_2 \xrightarrow{E_2} AB + AB$ $A_2B_2 \xrightarrow{E_{2B}} A_2B + B$ $A_3B \xrightarrow{E_{A_3B}} A_2B + A_1$	$A_2B_2 + NO_3^- \xrightarrow{k_c} A_2B_2^- \xrightarrow{fast} A_2^-$ $AB + NO_3^- \xrightarrow{k_c} AB^- \xrightarrow{fast} A_1^-$ $A_1 + NO_3^- \xrightarrow{k_c} A_1^-$ $A_2B + NO_3^- \xrightarrow{k_c} A_2B^- \xrightarrow{fast} A_2^-$ $A_3B + NO_3^- \xrightarrow{k_c} A_3B^- \xrightarrow{E_{A_3B^-}} A_2^- + A_1B$ $N_4 + NO_3^- \xrightarrow{k_c} N_4^-$ $A_3B_3 + NO_3^- \xrightarrow{k_c} A_3^-B_3 \xrightarrow{fast} A_3^-B_2$ $A_3B_2 + NO_3^- \xrightarrow{k_c} A_3B_2^- \xrightarrow{E_{A_3B_2^-}} A_3B^-$	$A_1^- + A_1 \xrightarrow{k_c} A_2^-$ $A_2^- + A_1 \text{ or } AB \xrightarrow{k_c} A_3^-$ $A_1^- + A_2B \xrightarrow{k_c} A_3B^-$ $A_1^- + A_3B \xrightarrow{k_c} N_4^-$ $A_1^- + A_2B_2 \xrightarrow{k_c} A_3B_2^-$ $A_1^- + AB \xrightarrow{k_c} A_2B^- \xrightarrow{fast} A_2^-$

References:

- Berresheim, H., Elste, T., Plass-Dülmer, C., Eisele, F. L., and Tanner, D. J.: Chemical ionization mass spectrometer for long-term measurements of atmospheric OH and H₂SO₄, *International Journal of Mass Spectrometry*, 202, 91-109, 10.1016/s1387-3806(00)00233-5, 2000.
- Eisele, F. L., and Hanson, D. R.: First Measurement of Prenucleation Molecular Clusters, *The Journal of Physical Chemistry A*, 104, 830-836, 10.1021/jp9930651, 2000.
- Rosser, S., and de la Mora, J. F.: Vienna-Type DMA of High Resolution and High Flow Rate, *Aerosol Science and Technology*, 39, 1191-1200, 10.1080/02786820500444820, 2005.
- Ude, S., and de la Mora, J. F.: Molecular monodisperse mobility and mass standards from electrosprays of tetra-alkyl ammonium halides, *Journal of Aerosol Science*, 36, 1224-1237, 10.1016/j.jaerosci.2005.02.009, 2005.
- Zhao, J., Eisele, F. L., Titcombe, M., Kuang, C., and McMurry, P. H.: Chemical ionization mass spectrometric measurements of atmospheric neutral clusters using the cluster-CIMS, *J. Geophys. Res.*, 115, D08205, 10.1029/2009jd012606, 2010.